



# Bacteriohopanetetrol-*x*: constraining its application as a lipid biomarker for marine anammox using the water column oxygen gradient of the Benguela upwelling system

Zoë R. van Kemenade<sup>1</sup>, Laura Villanueva<sup>1,2</sup>, Ellen C. Hopmans<sup>1</sup>, Peter Kraal<sup>1</sup>, Harry J. Witte<sup>1</sup>, Jaap S. Sinninghe Damsté<sup>1,2</sup>, Darci Rush<sup>1</sup>

<sup>1</sup>Department of Marine Microbiology and Biogeochemistry, NIOZ Royal Netherlands Institute for Sea Research, Den Burg, the Netherlands

<sup>2</sup>Department of Earth Sciences, Geochemistry, Faculty of Geosciences, University of Utrecht, Utrecht, the Netherlands

Correspondence to: Zoë R. van Kemenade (zoe.van.kemenade@nioz.nl)

**Abstract.** Interpreting lipid biomarkers in the sediment archive requires a good understanding of their application and limitations in modern systems. Recently it was discovered that marine bacteria performing anaerobic ammonium oxidation (anammox), belonging to the genus *Ca. Scalindua*, uniquely synthesize a stereoisomer of bacteriohopanetetrol ('BHT-*x*'). The ratio of BHT-*x* over total bacteriohopanetetrol (BHT; ubiquitously synthesized by diverse bacteria) has been suggested as a proxy for water column anoxia. As BHT has been found in sediments over 50 Myr old, BHT-*x* has the potential to complement and extend the sedimentary biomarker record of marine anammox, conventionally constructed using ladderane lipids. Yet, little is known about the distribution of BHT-*x* in relation to the distribution of ladderanes and to the genetic evidence of *Ca. Scalindua* in modern marine systems. Here, we investigate the distribution of BHT-*x* and the application of the BHT-*x* ratio in relation to distributions of intact polar (IPL) ladderane lipids, ladderane fatty acids (FAs) and *Ca. Scalindua* 16S rRNA genes in suspended particulate matter (SPM) from the water column, sampled across a large oxygen gradient in the Benguela upwelling system (BUS). In BUS SPM, high BHT-*x* abundances were constrained to the oxygen deficient zone on the continental shelf (at [O<sub>2</sub>] <45 μmol L<sup>-1</sup>, in all but one case). High BHT-*x* abundances co-occurred with high abundances of the *Ca. Scalindua* 16S rRNA gene (relative to the total number of bacterial 16S rRNA genes) and ladderane IPLs. At shelf stations with [O<sub>2</sub>] >50 μmol L<sup>-1</sup>, the BHT-*x* ratio was <0.04 (in all but one case). In apparent contradiction, ladderane FAs and low abundances of BHT and BHT-*x* (resulting in BHT-*x* ratio's >0.04) were also detected in oxygenated offshore waters ([O<sub>2</sub>] up to 180 μmol L<sup>-1</sup>), whereas ladderane IPLs were undetected. NL<sub>5</sub>-derived temperatures suggested that ladderane FAs in the offshore waters were not synthesized *in situ* but derived from warmer shelf waters. Thus, in sedimentary archives of systems with known lateral organic matter transport, such as the BUS, relative BHT and BHT-*x* abundances should be carefully considered. In such systems, a higher BHT-*x* ratio may act as a safer threshold for deoxygenation and/or *Ca. Scalindua* presence: in the BUS, at [O<sub>2</sub>] >50 μmol L<sup>-1</sup>, the BHT-*x* ratio was <0.18 at both off- and onshore sites (in all but one case) and a ratio >0.18 corresponded in all cases (except one) with the presence of *Ca. Scalindua* 16S rRNA genes. Lastly, when investigating *in situ* anammox, we highlight the importance of using ladderane IPLs over BHT-*x* and/or ladderane FAs; these latter compounds are more recalcitrant and may derive from transported fossil anammox bacteria remnants.

## 1 Introduction

Anaerobic ammonium oxidizing (anammox) bacteria are a deep branching monophyletic group belonging to the order *Planctomycetales* (Strous et al., 1999). Anammox bacteria oxidize ammonium (NH<sub>4</sub><sup>+</sup>) to dinitrogen gas (N<sub>2</sub>), using nitrite (NO<sub>2</sub><sup>-</sup>) as an electron acceptor (Van de Graaf et al., 1995; 1997). Of the five known anammox genera, only '*Candidatus Ca. Scalindua*' has been found in open marine environments, of which the first identified species was '*Ca. Scalindua sorokinii*' in the Black Sea (Kuypers et al. 2003; Schmid et al. 2003). Since then, studies have found *Ca. Scalindua* spp. to also be present in numerous oxygen minimum zones (OMZs) worldwide (Schmid et al., 2007; Woebken et al., 2007; Villanueva et al. 2014),



40 where they are responsible for major losses of fixed nitrogen (*e.g.* Thamdrup et al., 2006; Schmid et al., 2007; Jensen et al., 2008; Lam et al., 2009). Although permanent OMZs (defined as  $O_2 < 20 \mu\text{mol L}^{-1}$ , reaching  $1 \mu\text{mol L}^{-1}$  in the core) constitute only ~8% of the total oceanic area (Paulmier & Ruiz-Pino, 2009), they are responsible for 20–50% of the total global nitrogen (N) loss (Gruber & Sarmiento, 1997; Codispoti et al., 2001; Gruber, 2004). Climate models predict that OMZs will expand both spatially and temporally (Oschlies et al., 2018), thereby increasing the potential of fixed N-loss processes, such as  
 45 anammox, in marine systems (Breitburg et al. 2018), hereby altering the biogeochemistry of the oceans.

To constrain past and present N cycle variations, lipid biomarkers can be employed (see Rush and Sinninghe Damsté, 2017 for a review). Subsequently, biomarker information can be applied for predictions of future N cycling variations (*e.g.* Monteiro et al., 2012). Anammox bacteria uniquely synthesize ladderane fatty acids (FAs) and ladderane glycerol monoethers, which contain three or five linearly concatenated cyclobutane rings, designated respectively as [3]- and [5]-ladderanes  
 50 (Sinninghe Damsté et al., 2002, 2005; Fig. 1b). These biomarker lipids have been used to detect anammox bacteria in the natural environment (*e.g.* Kuypers et al., 2003; Hamersley et al., 2007; Jaeschke et al., 2010). Intact polar lipid (IPL)-containing ladderanes have also been used as biomarker lipids for the presence of anammox bacteria in marine waters and sediments (*e.g.* Jaeschke et al., 2010; Brandsma et al., 2011; Pitcher et al., 2011). Ladderane IPLs consist of two hydrocarbon chains, at least one being a [3]- or [5]- ladderane, esterified or ether-bound to a glycerol moiety, which is in turn bound to a polar headgroup  
 55 (phosphocholine ‘PC’, phosphoethanolamine ‘PE’ or phosphoglycerol ‘PG’; Boumann et al., 2006; Rattray et al., 2008). Ladderane IPLs are thought to reflect living or recently dead anammox cells (Jaeschke et al., 2009a; Jaeschke et al., 2010; Brandsma et al., 2011; Bale et al., 2014), as they rapidly degrade after cell lysis (*i.e.*, by headgroup cleavage; Harvey et al., 1986). By contrast, the oldest reported ladderane FAs were found in 140 kyr old sediments underlying the Arabian Sea OMZ (Jaeschke et al. 2009b). However, partly due to the steric strain on the cyclobutane moieties, ladderane FAs degrade during  
 60 diagenesis. Thus, in order to constrain the role of anammox in the N cycle during earlier time periods, a more recalcitrant biomarker is required.

Recently, a rare stereoisomer (BHT-*x*) of the ubiquitous bacteriohopanetetrol (BHT), a pentacyclic  $C_{30}$  triterpenoid linked to a tetrafunctionalised side chain, was reported to be uniquely synthesized by marine anammox, *Ca. Scalindua* (Rush et al., 2014; Schwartz-Narbonne et al., 2020; Fig. 1a). BHTs belong to the family of bacteriohopanepolyols (BHPs), which are  
 65 biological precursors of hopanoids, ubiquitously found in the geological record (Ourisson & Albrecht, 1992). Intact BHPs have been found in sediments over 50 Myr old (van Dongen et al. 2006; Talbot et al. 2016; Rush et al., 2019). BHT-*x* was found to have the same distribution as ladderane FAs in sediments of Golfo Dulce, an anoxic marine enclosure in Costa Rica (Rush et al., 2014), testifying to its potential application as anammox marker. Moreover, since BHT is ubiquitous and the BHT-*x* stereoisomer was only found in low oxygen settings, Saénz et al (2011) had earlier proposed the ratio of BHT-*x* over  
 70 total BHT (BHT-*x* ratio) to be a proxy for water column deoxygenation ( $[O_2] < 50 \mu\text{mol L}^{-1}$ ). These studies show the potential of BHT-*x* to complement and extend the ladderane biomarker record.

To better interpret BHT-*x* as a biomarker in the sedimentary record, either as an indicator for the presence of marine anammox, *Ca. Scalindua* spp., or as a proxy for water column deoxygenation, it is imperative to establish how BHT-*x* is distributed in modern marine oxygen-depleted systems. In this study, we combine measurements of BHT-*x*, ladderane lipids  
 75 (both as IPLs and FAs) and 16S rRNA marker genes in suspended particulate matter (SPM) across a redox gradient in the water column of the Benguela upwelling system (BUS). The BUS, located along the southwest African continental margin (Fig. 2a), supports one of the most productive regions in the world. The high productivity on the broad but shallow continental shelf results in a perennial OMZ off-shelf, between ~200-500 m below sea surface (mbss). Additionally, annual variation in upwelling intensity leads to a seasonal, on-shelf oxygen deficient zone (ODZ; here defined as  $[O_2] < 5 \mu\text{mol L}^{-1}$  in bottom  
 80 waters), which develops in late austral summer (Chapman and Shannon, 1987; Bailey et al., 1991; Mercier et al., 2003; Ekau and Verheye, 2005; Bruchert et al., 2006; Mohrholz et al., 2008). Previous research has indicated that in the BUS, anammox is responsible for major losses of bioavailable nitrogen (Kuypers et al. 2005; Kalvelage et al., 2011). The BUS therefore is an



optimal modern marine system to assess the distribution of BHT-*x* in relation to that of ladderane IPLs, ladderane FAs and *Ca. Scalindua* 16S rRNA gene sequences, across a large water column oxygen gradient.

85

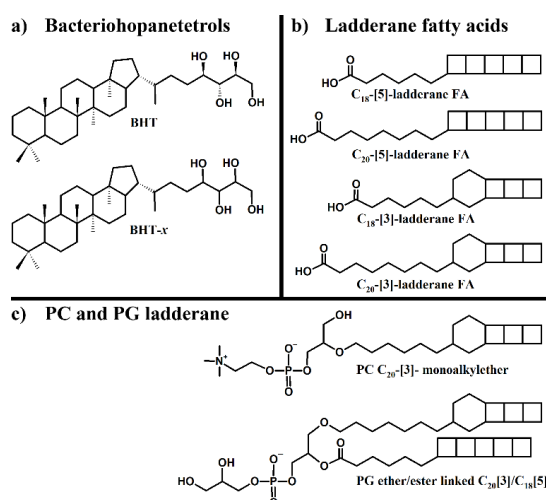


**Figure 1.** Structures of lipid biomarkers used in this study: a) Bacteriohopane-17 $\beta$ , 21 $\beta$ (H), 22R, 32R, 33R, 34S, 35-tetrol (BHT), ubiquitously synthesized by bacteria, and bacteriohopanetetrol stereoisomer (BHT-*x*), with an unknown stereochemistry of the tetrafunctionalised side-chain, uniquely synthesized by marine anammox bacteria; b) ladderane fatty acids (FAs) with 5 or 3 cyclobutane moieties and 18 or 20 carbon atoms; and c) Intact polar lipid ladderanes PC C<sub>20</sub>[3]-monoalkylether ('PC ladderane') and PG ether/ester linked C<sub>20</sub>[3]/C<sub>18</sub>[5] ('PG ladderane').

## 2 Materials and methods

### 2.1 Hydrographic setting

The BUS is located off the southwest African coast, where the cold and nutrient rich waters of the Benguela current are upwelled through a combination of wind-driven Ekman transport and collision with the African continental shelf. The studied area is situated in the northern part of the BUS (16–26°S and 10–16°E; Fig. 2a). Here, changes in the offshore wind field, which affect upwelling and hence primary production, result in seasonal variations and movements of the oxygen depleted waters (Chapman and Shannon, 1987). The northern border of the BUS is delineated by the dynamic Angolan Benguela Front (ABF; ~16–20°S), where the warm and oligotrophic waters of the Angola current (AC), transporting the oxygen poor (<45  $\mu\text{mol L}^{-1}$ ) South Atlantic Central Water (SACW) southwards, converge with the cold and nutrient-rich waters of the equatorward Benguela current (BC). Seasonal variations in the intensity of the AC and the BC control dissolved oxygen concentrations in the BUS (Mohrholz et al., 1999; Bruchert et al., 2006; Fig. 2a). This results in a near permanently present OMZ located off the continental shelf (~200–500 mbss; [O<sub>2</sub>] ~20–50  $\mu\text{mol L}^{-1}$ ) and a seasonally variable oxygen deficient zone (ODZ) on the continental shelf (~50 mbss to seafloor; [O<sub>2</sub>] < 5  $\mu\text{mol L}^{-1}$ ), where the most severe oxygen depletion occurs during late austral summer (Chapman and Shannon, 1987; Bailey et al., 1991; Mercier et al., 2003; Ekau and Verheye, 2005; Bruchert et al., 2006; Mohrholz et al., 2008). In the south, the northern BUS is bordered by the Lüderitz upwelling cell around ~26°S (Boyer et al., 2000).

### 2.2 Sample collection

Between January and March 2019, two consecutive research expeditions in the Namibian BUS were undertaken with the *R/V Pelagia* (64PE449 and 64PE450). At this time, the low-oxygen waters of the SACW reached their maximum southward extension (Chapman and Shannon, 1987), which, combined with limited cross-shore bottom-water ventilation at the start of the annual upwelling cycle, led to severe oxygen depletion (Mohrholz et al., 2008). Sampling was performed at various water depths at 13 stations (11°22' 36.5"-14°47'34.8" E and 17°16'38.3"-25°12'25.0" S; Fig. 2a; Table 1), covering a large range in water column oxygen concentrations (Fig. 2b). From here on, the deeper stations (>300 mbss stations 1, 2, 8, 9, 59), sampled



in the OMZ off the continental shelf will be termed ‘offshore stations’, whereas the shallower stations (<120 mbss; stations 3, 4, 5, 6, 10, 18, 117, 140) sampled in the ODZ on the continental shelf will be termed ‘shelf stations’ (Table 1). At each station, physical parameters of the water column were recorded with a Sea-Bird SBE911+ conductivity-temperature-depth (CTD) system. The CTD was equipped with an additional SBE 43 oxygen electrode (Sea-Bird Electronics, WA, USA) to measure dissolved oxygen (detection limit of 1-2  $\mu\text{mol L}^{-1}$ ). A NIOZ-made Rosette sampler of 24 x 12L Niskin bottles with hydraulically controlled butterfly lids was used to collect water for nutrient and DNA analysis. An overpressure of  $\text{N}_2$  gas of ~0.5 bar was applied to the Niskin bottles to collect water without introducing oxygen. Water samples for DNA analysis were collected into pre-cleaned acid-washed Nalgene bottles. Ca. 2 L of water was filtered over 0.2  $\mu\text{m}$  pore diameter Millipore Sterivex filters from Nalgene bottles kept on ice in a climate-controlled container set at 4°C. 2 mL of RNALater (RNA protect bacteria reagent, Qiagen) was applied to the Sterivex cartridges, which were then sealed with parafilm and stored at -20 °C until further processing. Suspended particulate matter (SPM) for lipid analysis was collected using four McLane Large Volume Water Transfer System Sampler (WTS-LV) in situ pumps (McLane Laboratories Inc., Falmouth, MA, USA). Water was filtered onto pre-ashed GF75 grade glass fibre filters of 0.3  $\mu\text{m}$  pore size and 142 mm diameter (Advantec MFS, Inc., USA). Filters were wrapped in aluminium foil and stored at -80 °C until further processing. Water column sampling depths were chosen based on the CTD profiles, focusing around and below the redoxcline (Table S1).

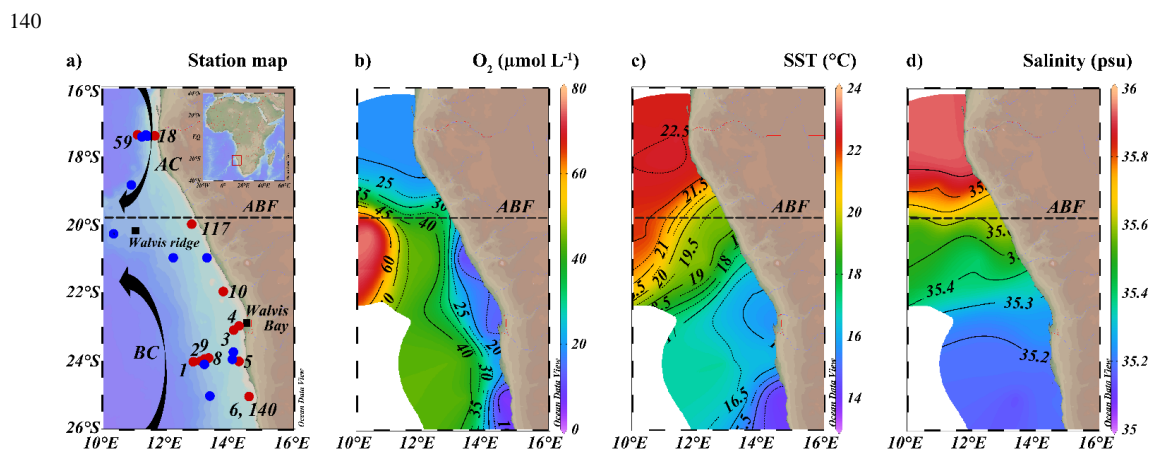


**Figure 2:** a) Map of sampled stations during expeditions 64PE449 (27/01/19-14/02/19) and 64PE450 ((15/02/19-10/03/19), with station dots colour coded according to sampling activities; CTD casts and nutrients (blue), and CTD casts and nutrients plus DNA and SPM sampling (red). Numbers indicate station labels of red dots. b) minimum observed oxygen concentration in water column, c) sea surface temperature (SST) and d) maximum observed salinity in water column. AC: Angolan current, BC: Benguela current, ABF: Angolan Benguela Front (~19.8°S). Maps were created in ODV using the ETOP01\_2min global tiles map 150x75 weighted average gridding (Schlitzer, R, Ocean Data View, <https://odv.awi.de>, 2019).

### 2.3 Nutrient analysis

Samples for nutrient analysis were sub-sampled from the Niskin bottles with pre-flushed 60 mL high-density polyethylene syringes with a three-way valve. Samples for  $\text{PO}_4^{3-}$ ,  $\text{NO}_2^-$ ,  $\text{NO}_3^-$  and  $\text{NH}_4^+$  analysis were filtered over a combined 0.8-0.2  $\mu\text{m}$  Supor Membrane Acrodisc PF syringe filter (PALL Corporation, NY, USA) into pre-rinsed 5 mL polyethylene vials and analysed onboard with an autoanalyzer (QuAAtro39 Gas Segmented Continuous Flow Analyser, Seal Instruments). Detection limits for  $\text{PO}_4^{3-}$ ,  $\text{NO}_2^-$ ,  $\text{NO}_3^-$  and  $\text{NH}_4^+$  were 0.005, 0.003, 0.015 and 0.019  $\mu\text{mol L}^{-1}$ , respectively. The fixed inorganic nitrogen deficit was calculated as:

$$N \text{ deficit} = 16 \times [\text{PO}_4^{3-}] - ([\text{NO}_3^-] + [\text{NO}_2^-] + [\text{NH}_4^+]) \quad (1)$$



in which 16 reflects the Redfield ratio of N:P (Redfield et al., 1960).

160

**Table 1.** Sampling date, cruise name, station label, coordinates and sediment depth (mbss), during expeditions 64PE449 and 64PE450. Stations are grouped according to their location on the continental shelf. Location is 'shelf' when sediment depth is <120 mbss, or 'offshore' when sediment depth is >300 mbss.

Date	Cruise	Station	Latitude (°S)	Longitude (°E)	Depth (mbss)	Location
01-02-2019	64PE449	3	23.096	14.129	120	Shelf
06-02-2019	64PE449	4	23.011	14.244	105	Shelf
07-02-2019	64PE449	5	24.020	14.303	100	Shelf
08-02-2019	64PE449	6*	25.072	14.596	100	Shelf
12-02-2019	64PE449	10	21.968	13.793	103	Shelf
19-02-2019	64PE450	18	17.409	11.635	100	Shelf
01-03-2019	64PE450	117	20.001	12.823	105	Shelf
07-03-2019	64PE450	140*	25.072	14.596	100	Shelf
03-02-2019	64PE449	1	24.056	12.843	1500	Offshore
04-02-2019	64PE449	2	24.042	13.127	720	Offshore
10-02-2019	64PE449	8	23.961	13.227	324	Offshore
11-02-2019	64PE449	9	23.962	13.226	407	Offshore
25-02-2019	64PE450	59	17.277	11.377	1000	Offshore

\*denotes same station location, sampled 27 days apart

## 165 2.4. Lipid extraction and analysis

### 2.4.1 Modified Bligh and Dyer extraction

Freeze-dried filters were extracted four times using a modified Bligh and Dyer extraction (BDE) method (Bligh and Dyer, 1959; Sturt et al., 2004; Bale et al., 2021). The filters were cut in  $\pm 1 \times 1$  cm pieces, and ultrasonically extracted (10 min) using a solvent mixture of 2:1:0.8 (v:v:v) methanol (MeOH), dichloromethane (DCM) and phosphate buffer, sonicated for 10 min and centrifuged for 2 min at 3000 rpm. The supernatant was then transferred to another tube, while the residue was re-extracted thrice, in which the last two times the phosphate buffer was replaced with a trichloroacetic acid solution. Phase separation between the solvent layer and aqueous layer was induced by adding additional DCM and phosphate buffer to obtain a ratio of 1:1:0.9 (v:v:v). The bottom DCM layer, containing the lipid extract, was collected, while the aqueous layer was washed two more times with DCM. The combined DCM layers were dried under  $N_2$  gas. This extraction method was also performed on freeze-dried biomass from a *Ca. Scalindua brodae* enrichment culture, obtained from an anoxic sequencing batch reactor at Radboud University, Nijmegen, The Netherlands (described in Schwartz-Narbonne et al., 2019).

### 2.4.2 BHP and IPL analyses

Deuterated diacylglyceryltrimethylhomoserine (DGTS D-9; Avanti® Polar Lipids, USA) was added as an internal standard to BDE aliquots. Aliquots were then filtered over 4 mm True generated cellulose syringe filters (0.45  $\mu$ m, BGB, USA) and re-dissolved in a MeOH: DCM solution of 9:1 (v:v) before analysis. Filtered aliquots were analysed on an Agilent 1290 Infinity I ultra high performance liquid chromatographer (UHPLC) equipped with a thermostatted auto-injector and column oven, coupled to a Q Exactive Orbitrap MS with an Ion Max source and heated electrospray ionisation probe (HESI; ThermoFisher Scientific, Waltham, MA). Separation was accomplished with an Acquity BEH  $C_{18}$  column (2.1 $\times$ 150 mm, 1.7  $\mu$ m, Waters)



maintained at 30°C. An eluant of (A) MeOH/H<sub>2</sub>O/formic acid/14.8 M NH<sub>3</sub>aq with a ratio of 85:15:0.12:0.04 (v:v:v:v) and  
 185 (B) IPA/MeOH/formic acid/14.8 M NH<sub>3</sub>aq with a ratio of 50:50:0.12:0.04 (v:v:v:v) was used, with a flow rate of 0.2 mL  
 min<sup>-1</sup>. The elution program was set at: 5% B for 5 min, followed by a linear gradient to 40% B at 12 min and then to 100% B  
 at 50 min, which was maintained until 80 min. Positive ion HESI settings were: capillary temperature, 300°C; sheath gas (N<sub>2</sub>)  
 pressure, 40 arbitrary units (AU); auxiliary gas (N<sub>2</sub>) pressure, 10 AU; spray voltage, 4.5 kV; probe heater temperature, 50°C;  
 S-lens 70 V. Lipids were detected using positive ion monitoring of *m/z* 350–2000 (resolution 70,000 ppm at *m/z* 200), followed  
 190 by data dependent MS<sup>2</sup> (resolution 17,500 ppm) of the ten most abundant ions and dynamic exclusion (for 6s) within 3 ppm  
 mass tolerance. An inclusion list with the calculated exact masses of 165 calculated BHPs was applied. Optimal fragmentation  
 was achieved with a stepped normalized collision energy of 22.5 and 40 (isolation width 1.0 *m/z*) for BHP analysis (Hopmans  
 et al., 2021) and 15, 22.5 and 30 (isolation width, 1.0 *m/z*) for IPL analysis (Bale et al., 2021). The Q Exactive Orbitrap was  
 calibrated every 48h using the ThermoScientific Pierce LTQ Velos ESI Positive Ion Calibration Solution. The summed mass  
 195 chromatograms of the ammoniated ([M+NH<sub>4</sub>]<sup>+</sup>; *m/z* 564.499) and sodiated ([M+Na]<sup>+</sup>; *m/z* 569.454) adducts of BHT(-x) were  
 integrated within 3 ppm mass accuracy. The BHT-x ratio was then calculated as:

$$BHT - x \text{ ratio} = \frac{BHT-x}{(BHT+BHT-x)} \quad (2)$$

200 All ladderane IPLs reported by Rattray et al., 2008 were evaluated in the BUS SPM samples and a *Ca. Scalindua brodae*  
 enrichment culture (see Table S4 for exact masses). Only PC C<sub>20</sub>[3] monoalkylether (from here on termed ‘PC ladderane’) and  
 an ether-ester PG C<sub>20</sub>[3]-C<sub>18</sub>[5] (from here on termed ‘PG ladderane’) were detected in the BUS SPM samples (Fig. 1c). For  
 the PC ladderane, the exact ion mass was used for integration ([M]<sup>+</sup>; *m/z* 530.361). For the PG ladderane, the combined  
 protonated ([M+H]<sup>+</sup>; *m/z* 775.491) and ammoniated ([M+NH<sub>4</sub>]<sup>+</sup>; *m/z* 792.517) adduct was used for integration (within 3 ppm  
 205 mass accuracy). BDE of the *Ca. S. brodae* enrichment culture (containing both ladderane IPLs and BHT-x) was used as a  
 quality control sample in each sequence run. Due to a lack of commercially available quantification standards for BHT(-x) and  
 ladderane IPLs, abundances are reported as the peak area response (response unit, ru) per litre of filtered water. Although this  
 does not allow for quantification of absolute concentrations, it does allow for quantification of the relative abundances, as the  
 response factor should be identical across the sample set.

#### 210 2.4.3 Ladderane fatty acids

SPM from stations 6, 140 and 2 were additionally analysed for ladderane FAs. BDE aliquots were saponified by adding 2 ml  
 of KOH (1 M in 96% MeOH) and refluxing for 1 h. Then, 2 mL of bidistilled water was added and the pH was adjusted to 3  
 with 1:1 HCL:MeOH (v:v). To collect the fatty acid fraction, 2 mL of DCM was added, after which the tube was sonicated for  
 5 min and centrifuged for 2 min at 3000 rpm. The fatty acid fraction (DCM layer) was collected, and the procedure was  
 215 repeated two more times. Fatty acid fractions were then dried over a sodium sulfate (Na<sub>2</sub>SO<sub>4</sub>) column. The fractions were then  
 methylated using diazomethane to convert FAs into their corresponding fatty acid methyl esters (FAMES). To remove  
 polyunsaturated fatty acids (PUFAs), extracts were dissolved in DCM and eluted over a silver nitrate (AgNO<sub>3</sub>) impregnated  
 silica column. Lastly, the FAME fractions were filtered through a 0.45 µm PTFE filter (BGB, USA) using acetone.

#### 2.4.4 Ladderane fatty acid analysis

220 Purified FAME fractions were analysed on an Agilent 1290 Infinity I ultra high performance liquid chromatographer (UHPLC)  
 equipped with a thermostatted auto-injector and column oven, coupled to a Q Exactive Plus Orbitrap MS, with an atmospheric  
 pressure chemical ionization (APCI) probe (Thermo Fischer Scientific, Waltham, MA). Separation was realised with a  
 ZORBAX Eclipse XDB C<sub>18</sub> column (Agilent, 3.0×250 mm, 5 µm), maintained at 30°C. MeOH was used as an eluant at 0.18



ml min<sup>-1</sup> with a total run time of 20 min. Optimal APCI source settings were determined using a qualitative standard mixture of [3]- and [5]-ladderane FAMES. Positive ion APCI source settings were: corona discharge current, 2.5 µA; source CID, 10 eV; vaporizer temperature, 475°C; sheath gas flow rate, 50 arbitrary units (AU); auxiliary gas flow rate, 30 AU; capillary temperature, 300°C; S-lens, 50 V. A mass range of *m/z* 225–380 was monitored (resolution 140,000 ppm), followed by a data-dependent MS<sup>2</sup> (resolution 17,500 ppm at *m/z* 200), in which the ten most abundant masses in the mass spectrum were fragmented successively (stepped normalized collision energy 20, 25, 30). An inclusion list containing the exact masses of C<sub>14-24</sub> [3]- and [5] ladderane FAMES was used. Mass chromatograms (within 5 ppm mass accuracy) of the protonated molecules ([M+H]<sup>+</sup>) were used to integrate C<sub>18</sub>[3]-, C<sub>18</sub>[5]-, C<sub>20</sub>[3]- and C<sub>20</sub>[5]-ladderane FAMES (*m/z* 291.232, 289.216, 319.263, 317.248, respectively). Ladderane FAMES were quantified by external calibration curves of isolated standards of the C<sub>20</sub>[3]- and [5] ladderane FAMES (Hopmans et al., 2006; Rattray et al., 2008; Rush et al., 2011;). The index of ladderane lipids with 5 cyclobutane rings (NL<sub>5</sub>) was calculated to quantify the trends in ladderane chain lengths with respect to temperature, using:

$$NL_5 = \frac{C_{20}[5]ladderane\ FA}{C_{18}[5]ladderane\ FA + C_{20}[5]ladderane\ FA} \quad (3)$$

Following, the relationship between NL<sub>5</sub> and temperature is then given by:

$$NL_5 = 0.2 + \frac{0.7}{1 + e^{-\left(\frac{T-16.3}{1.5}\right)}} \quad (4)$$

with temperature (T) in °C (Rattray et al., 2010).

## 2.5. DNA extraction and phylogenetic analysis

Millipore® Sterivex™ filters were extracted for DNA using the Qiagen DNeasy Powersoil kit<sup>□</sup>. PCR reactions of the DNA templates were conducted with the Qiagen<sup>□</sup> PCR reagents (Taq PCR Master Mix Kit). The universal prokaryotic primer pair, forward 515F-Y and reverse 926R (Parada et al. 2015) was used to target the V4-V5 small subunit ribosomal RNA region, and was modified with different 12 nucleotide barcodes at both the forward and reverse primer. The 515-Y/926R primer pair has been found to successfully target *Ca. Scalindua* (e.g. Yang et al., 2020) and is reported to reflect marine community compositions well (Parada et al., 2015). Reagents were mixed with fifty times diluted DNA template (2 µL) by addition of: 11.75 µL Nuclease free water, 5 µL 5x Qiagen Phusion buffer, 2 µL dNTPs (2.5 mM), 3 µL of 515F-Y/926R primer pair (4 µmol L<sup>-1</sup>), 1 µL BSA (20 mg ml<sup>-1</sup>) and 0.25 µL Taq polymerase (5 units µL<sup>-1</sup>). Negative controls were included during extractions and PCR reactions. Amplification was performed using the following PCR program: 30s at 98°C (1 cycle), 10s at 98° followed by 20s at 50°C and 30s at 72°C (30 cycles), 7 min at 72°C (1 cycle) and ending with 5 min at 4°C. To quantify DNA concentrations of the PCR reagents, PCR products were mixed with a Xylene Ficoll loading dye and loaded on a 2% agarose gel, together with a home-made *Escherichia coli* quantification standard dilution series (20, 10 and 1 ng µL<sup>-1</sup>). Gel electrophoresis was performed for 1h at 75 V. After, the gel was stained with Ethidium bromide. Gels were imaged using GeneSys (lightning, TLUM – Mid Wave; filter, UVO32). The 400 bp bands were then quantified using the ‘QuickQuant’ option. Following quantification, all PCR products were pooled in equimolar amounts (40 ng DNA per sample) and loaded on a 2% gel stained with SYBRsafe®. The 400 bp band was extracted from the gel using the QIAquick® PCR Gel Extraction Kit. Concentration of the pooled PCR product (20 ng µL<sup>-1</sup>) was quantified using Qbit (Thermo Fisher Scientific Inc.). Library preparation was performed with a 16S V4-V5 library preparation kit and sequencing with an Illumina MiSeq 2x300 bp sequencing platform (Illumina, San Diego, CA) at the University of Utrecht Sequencing Facility (USEQ, the Netherlands).

The prokaryotic 16S rRNA gene amplicon sequences were analysed using the *Cascabel* data analysis pipeline (Abdala Asbun et al. 2019). Raw forward and reverse reads were merged using PEAR (Zhang et al. 2015). Barcode reads were



demultiplexed using QIIME (Caporaso et al. 2010), allowing a maximum of 2 barcode mismatches, a maximum of 5  
 265 consecutive low-quality base calls and a maximum unaccepted Phred quality score of 19. Reads were then filtered based on  
 length using the values of the median distribution, with an offset of 10 bp. Sequences were dereplicated with VSEARCH, and  
 subsequently clustered to operational taxonomic units (OTUs) using the UCLUST algorithm in QIIME, with a 97% threshold.  
 From each OTU, the most abundant sequence was picked as representative with QIIME (Caporaso et al, 2010). Taxonomy  
 was assigned based on the SILVA database (SSU 138 Ref NR 99), using the VSEARCH tool. OTUs representative of the  
 270 order Brocadiales (to which *Ca. Scalindua* spp. belong) were extracted with QIIME using filter\_taxa\_from\_otu\_table.py. The  
 filtered sequences were imported in the SILVA NR99 SSU 138 Ref database using the ARB parsimony tool in the ARB  
 software package (ARB SILVA, Germany) to assess the phylogenetic affiliation of the partial 16S rRNA gene sequences.  
 Affiliated sequences were checked for homology and imported in MEGAX using the BLAST search query (Madden, 2002;  
 Kumar et al. 2018). The twelve OTUs with the largest number of reads and 27 reference sequences were aligned, based on 422  
 275 bp, with the Clustal W alignment tool. A Kimura 2-parameter model with *Gamma* distributed sites was then used to calculate  
 pairwise distances between sequences and to create a maximum likelihood tree in MEGAX, using a bootstrap with 1,000  
 replicates and the maximum parsimony method to create the initial tree (Kimura, 1980; Kumar et al. 2018; Stecher et al. 2020).  
 To estimate the relative abundance of *Ca. Scalindua* spp. 16S rRNA reads in relation to the total amount of bacterial 16S rRNA  
 reads, relative *Ca. Scalindua* spp. reads were calculated for each sample (in % of total bacterial reads). Though this does not  
 280 allow for absolute quantification, it does allow for a comparison of relative abundances throughout the dataset of this study,  
 as all samples were processed and analysed in the same way.

## 2.6 Statistical analysis

A multivariate binomial regression was performed with anammox biomarker lipids and *Ca. Scalindua* 16S rRNA gene  
 amplicon sequences. 16S rRNA gene amplicon sequences were used dichotomously, defined as either the presence or absence  
 285 of *Ca. Scalindua* assigned OTUs in a given sample. Pearson's correlations between anammox lipid biomarkers and the  
 physiochemical parameters were also investigated (Matlab, R2019a).

## 3 Results

### 3.1 Hydrography and seawater chemistry

The location of the ABF during the expedition was ~19.8°S, close to Walvis Ridge, where large horizontal gradients in sea  
 290 surface temperature (SST; temperatures integrated between 0-30 mbss) and salinity (measured at the halocline) were observed,  
 and surface isotherms and isohalines fanned out seawards (Figs. 2c and d). At the time of sampling, upwelled waters from the  
 BC were clearly distinguishable at the stations south of the ABF (St. 1-6, 10, 117 and 140; 20°S-26°S), where SST and salinity  
 are relatively low, ranging between 12.9-19.3°C and 35.1-35.6 psu, respectively (Table S1). Offshore (bottom depth ~300-  
 1500 mbss), a weak OMZ was present between ~100-500 mbss, with [O<sub>2</sub>] depletion down to ~40 µmol L<sup>-1</sup>. In the shallow  
 295 waters on the continental shelf (bottom depth <120 mbss) an ODZ was present, with [O<sub>2</sub>] decreasing rapidly with depth from  
 30 mbss onwards, with nearly anoxic waters ([O<sub>2</sub>] ~1.5-5.5 µmol L<sup>-1</sup>) below ~50-80 mbss. The strongest oxygen depletion was  
 found at the shallowest stations (<100 mbss; St. 4, 5, 6, 10, 117 and 140), while at the slightly deeper shelf station 3 (~120  
 mbss), [O<sub>2</sub>] in bottom waters were not lower than ~20 µmol L<sup>-1</sup> (Fig. 3c). The influence of the AC was apparent at stations  
 north of the ABF (Sts. 18 and 59), where SST and salinity are relatively high (Figs. 2c-d), ranging between 16.9-22.9°C and  
 300 35.7-35.9 psu, respectively (SM, Table S1). In these waters, [O<sub>2</sub>] declined to ~20 µmol L<sup>-1</sup> between ~50-500 mbss (Fig. 3c, j).  
 During the expeditions, nutrient concentrations in the BUS ranged between: 0.0-4.9 µmol L<sup>-1</sup> for NO<sub>2</sub><sup>-</sup>, 0-40 µmol L<sup>-1</sup> for NO<sub>3</sub><sup>-</sup>  
 , and 0.1-9.8 µmol L<sup>-1</sup> for NH<sub>4</sub><sup>+</sup> (Table S2; Figs. 3d-f, k-m). Nearly all sampled stations exhibited an N deficit (see equation  
 1) throughout the water column, with the strongest deficit being observed at the shelf stations. The N deficit was highest at St.



6, reaching a deficit of  $\sim 49 \mu\text{mol L}^{-1}$  at 85 mbss. When St. 6 was resampled in March (St. 140), the deficit had decreased to a maximum of  $\sim 23 \mu\text{mol L}^{-1}$  at 10 mbss. The only station in the BUS where no N deficit was observed was St. 117.

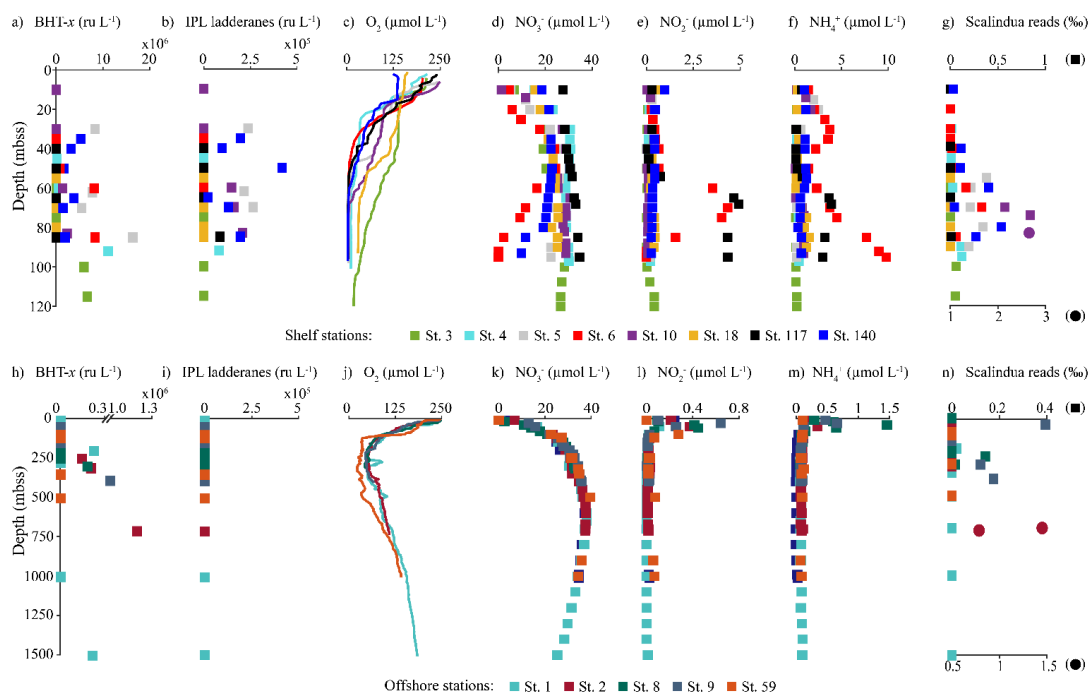


**Figure 3.** Concentration and relative abundance profiles in the water column of the BUS at shelf (top panels) and offshore (bottom panels) stations. (a, h) BHT-*x* abundance ( $\text{ru L}^{-1}$ ), (b, i) IPL ladderane abundance ( $\text{ru L}^{-1}$ ), concentrations of (c, j) oxygen [ $\text{O}_2$ ], (d, k) nitrate [ $\text{NO}_3^-$ ], (e, l) nitrite [ $\text{NO}_2^-$ ], (f, m) ammonium [ $\text{NH}_4^+$ ], (g, n) Relative abundance of *Ca. Scalindua* spp. reads in permille of total bacterial reads (NB circles are plotted on bottom x-axis with a different scale).

## 3.2 Anammox lipid biomarkers

### 3.2.1 BHT and BHT-*x* abundances and ratio

BHT was found in all SPM samples, except one (St. 117, 40 mbss). BHT abundance ranged between  $1.0 \times 10^5$ – $2.1 \times 10^8 \text{ ru L}^{-1}$  at the shelf stations and between  $1.1 \times 10^5$ – $1.8 \times 10^7 \text{ ru L}^{-1}$  at the offshore stations (Table S3). BHT-*x* was found exclusively in the southern part of the northern BUS. No BHT-*x* was observed at stations located near (St. 117) or north of the ABF (St. 18 and 59). When present, the BHT-*x* abundance ranged from  $1.4 \times 10^5$ – $1.6 \times 10^7 \text{ ru L}^{-1}$  (Figs. 3a, h; Table S3). At the southern stations located on the shelf (St. 3, 4, 5, 6, 10 and 140), BHT-*x* was observed at all stations below  $\sim 30$  mbss. At these stations, the BHT-*x* abundance ranged between  $2.3 \times 10^5$ – $1.6 \times 10^7 \text{ ru L}^{-1}$ . At the southernmost shelf station, when sampled in February (St. 6), BHT-*x* was observed between 50–85 mbss, increasing in abundance from  $8.5 \times 10^5 \text{ ru L}^{-1}$  at 50 mbss to  $8.3 \times 10^6 \text{ ru L}^{-1}$  at 85 mbss. When sampled in March (St. 140), BHT-*x* was present at all sampled depths (35–85 mbss), ranging between  $1.5$ – $5.3 \times 10^6 \text{ ru L}^{-1}$  (Fig. 3a; Table S3). At the southern offshore stations (St. 1, 2, 8, and 9), BHT-*x* was present between  $\sim 200$ – $400$  mbss and in the bottom waters. Here, the abundance ranged between  $1.4 \times 10^5$ – $1.2 \times 10^6 \text{ ru L}^{-1}$  (Fig. 3h; Table S3). The BHT-*x* ratio (see equation 2) in the BUS water column ranged between 0.00–0.55 (Fig. 4, Table S3).

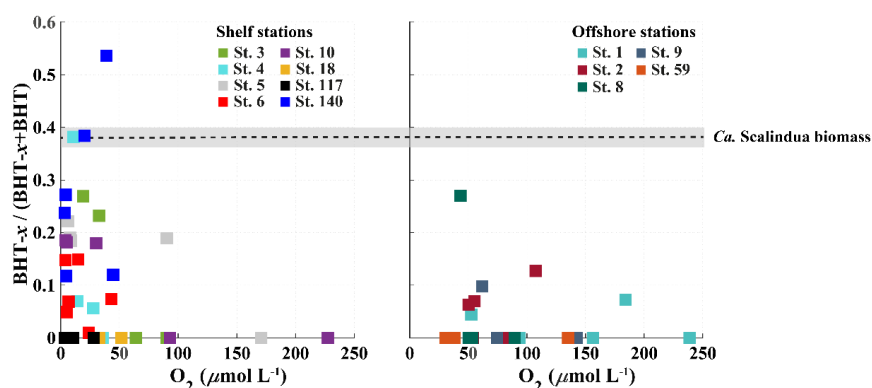


**Figure 4:** Scatter plots showing relationship between BHT- $x$  ratio ( $\text{BHT-}x/(\text{BHT}+\text{BHT-}x)$ ) and oxygen concentration ( $\mu\text{mol L}^{-1}$ ) for stations located on the shelf (left) and stations located offshore (right). The BHT- $x$  ratio observed in the *Ca. S. brodae* enrichment culture is indicated with the black dotted line at 0.38. The grey area corresponds to the standard deviation of the ratio ( $\pm 0.02$ ) between different HPLC/MS runs.

### 3.2.2 Ladderane IPLs

All ladderane IPLs observed in the *Ca. Scalindua brodae* enrichment culture (Table S4) and previously reported for *Ca. Scalindua* spp. (Rattray et al., 2008) were evaluated in the BUS SPM. The PC and PG ladderanes (section 2.4.2; Fig. 1c) were observed solely in SPM from a limited number of shelf stations located south of the ABF (St. 5, 10, 117 and 140), below ~30 mbss waters. Concentrations ranged between  $1.1 \times 10^4$ – $6.4 \times 10^5$  ru  $\text{L}^{-1}$  for the PG ladderane and between  $2.1 \times 10^4$ – $4.2 \times 10^5$  ru  $\text{L}^{-1}$  for the PC ladderane (Table S3). At station 5, PC and PG ladderanes were both present. At station 10, 117 and 140 the PG ladderane was less abundant or absent at the water column depths where the PC ladderane was found. From here on, their summed abundances are reported as ‘ladderane IPLs’.

### 3.2.3 Ladderane FAs

Ladderane FAs (i.e.  $\text{C}_{18}[3]$ -,  $\text{C}_{18}[5]$ -,  $\text{C}_{20}[3]$ - and  $\text{C}_{20}[5]$ -ladderane FAs; Fig. 5, Table S5) were analysed as FAMES in the SPM from an offshore station (St. 2) and of the southernmost shelf station, sampled in February (St. 6) and in March (St. 140). At the southernmost shelf station in February (St. 6; Fig 5b), highest ladderane FA concentrations were observed at the deepest sampling depth (85 mbss,  $0.14 \text{ ng L}^{-1}$ ). Concentrations an order of magnitude lower were found at the oxycline (30 mbss;  $0.02 \text{ ng L}^{-1}$ ) and at 60 mbss ( $0.03 \text{ ng L}^{-1}$ ), while no ladderane FAs were observed at 35 or 40 mbss. At this location in March (St. 140; Fig 5c), ladderane FAs were present throughout the low oxygen water column (35–85 mbss), with total concentrations ranging between  $0.02$ – $0.06 \text{ ng L}^{-1}$ . At the offshore Station 2 (Fig 5a), ladderane FAs were observed in the OMZ (125 and 250 mbss) and the bottom water (710 mbss). The  $\text{NL}_5$  index was calculated for all SPM samples that contained both  $\text{C}_{20}[5]$  and  $\text{C}_{18}[5]$  FAs (Table S5). For Station 6 and 140, the  $\text{NL}_5$  index ranged between  $0.18$ – $0.40$ . For Station 2, the  $\text{NL}_5$  was  $0.87$  at 250 mbss and  $0.47$  at 710 mbss. No evidence was found for the presence of short chain biodegradation products (i.e.  $\text{C}_{14}[3]$ -,  $\text{C}_{14}[5]$ -,  $\text{C}_{16}[3]$ -,  $\text{C}_{16}[5]$ - ladderane FAs; Rush et al., 2011), nor  $\text{C}_{22-24}$ -ladderane FAs.

### 3.3 16S rRNA gene analysis

16S rRNA gene amplicon sequencing analysis based on a fragment of 422 bp was conducted on SPM collected at 13 stations from various water column depths, including the same or similar depths as analysed for lipids. A total of 10,283,136 bacterial reads were recovered from the BUS stations (excluding singletons), of which  $0.14\%$  could be taxonomically assigned to the genus *Ca. Scalindua* (Arb SILVA 132R database). These sequences were further analysed to assess the distribution and phylogeny of *Ca. Scalindua* in the BUS. Negative controls did not contain reads taxonomically assigned to *Ca. Scalindua* spp.

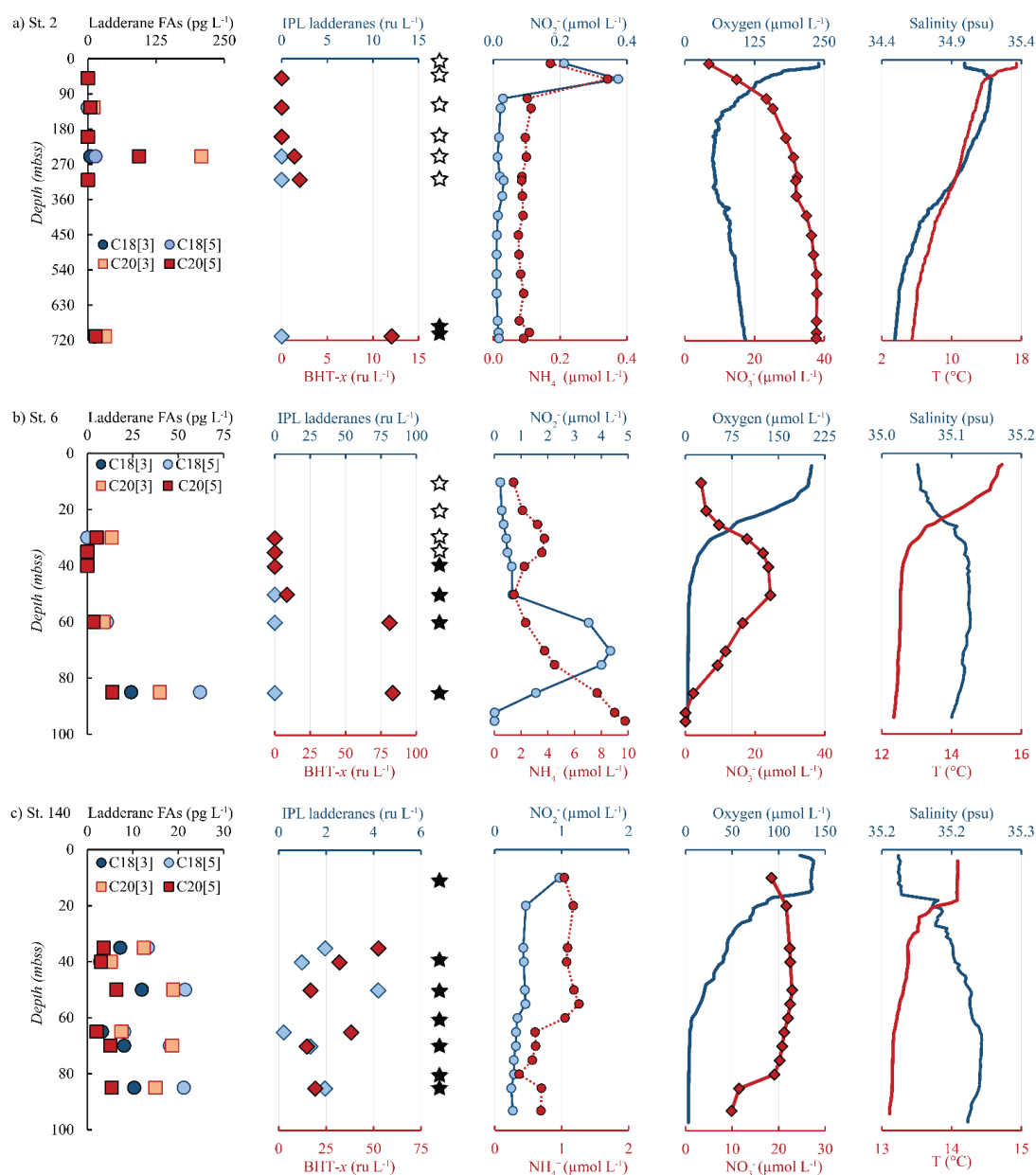


**Figure 5.** Water column depth profiles of stations (a) 2, (b) 6, and (c) 140, showing distributions of (from left to right) ladderane FAs ( $\text{pg L}^{-1}$ ), ladderane IPLs and BHT-x ( $\text{ru L}^{-1}$ ), nitrite and ammonium concentrations ( $\mu\text{mol L}^{-1}$ ), oxygen and nitrate concentrations ( $\mu\text{mol L}^{-1}$ ) and temperature ( $^{\circ}\text{C}$ ) and salinity (psu) profiles. Star symbols indicate water column depths where SPM was collected for DNA analysis. Filled stars represent depths where *Ca. Scalindua* spp. 16S rRNA gene sequences were detected. Stations 6 and 140 were sampled at the same location 27 days apart (St. 6 in February and St. 140 in March).

### 3.3.1 Distribution *Ca. Scalindua* spp. 16S rRNA sequences in the BUS

The relative abundances of *Ca. Scalindua* spp. 16S rRNA gene sequences in respect to the total amount of bacterial 16S rRNA gene sequences was calculated to estimate the distribution of *Ca. Scalindua* in the BUS (Figs. 3g, n). Sequences taxonomically



assigned to *Ca. Scalindua* spp. were detected in 11 out of 13 stations, in SPM collected at the shelf (<120 mbss; St. 3–6, 10 and 140) and at offshore stations (>300 mbss; St. 1, 2, 8 and 9) but were not detected at stations located north of the ABF (St. 18 and 55). At shelf stations (Fig. 3g), the relative *Ca. Scalindua* spp. gene read abundance ranged between 0–2.7‰, with highest abundances found below 50 mbss. In surface waters (<30 mbss), no *Ca. Scalindua* spp. 16S rRNA gene sequences  
 385 were detected, except at St. 140, where *Ca. Scalindua* spp. was present throughout the water column (0.03–0.53‰). At offshore stations, the relative abundance of *Ca. Scalindua* spp. 16S rRNA gene copies ranged between 0–1.5‰, with highest relative abundances found in bottom waters at St. 2 at 700 and 710 mbss (Fig. 3n). At offshore St. 1, 8 and 9, *Ca. Scalindua* spp. was detected between 50–390 mbss.

### 3.3.2 *Ca. Scalindua* phylogeny

390 *Ca. Scalindua* 16S rRNA reads (422 bp) were assigned to 66 operational taxonomic units (OTU 1–66) based on 97% sequence similarity (Table S6). Most of the *Ca. Scalindua* spp. reads (88%) could be assigned to twelve OTUs (OTU-1 to -12) ranging from the relatively most abundant to least abundant OTU (Fig. S1). To estimate the phylogenetic relationship of these 12 OTUs to *Ca. Scalindua* spp. sequences from other OMZs, a maximum likelihood tree was constructed with reference sequences from various other OMZs and anammox enrichment cultures (Fig. 6). In addition, the pairwise distances between these sequences  
 395 (based on 422 bp) were calculated (Table S7). The phylogeny of the BUS OTUs revealed a cluster of ten OTUs (OTUs 1–4 and 6–9, 11 and 12; Fig. 6), with an overall sequence identity of 96%. OTU-10 displays a relatively large evolutionary divergence (>12%; Fig. 6) and limited sequence identity (88%) to the other BUS OTUs. Highest sequence identity of the BUS OTU cluster is observed with environmental sequences isolated from the Guaymas deep sea hydrothermal vent sediment (98%) and the Black Sea suboxic waters (53 mbss; also 98%), which in turn both exhibited the highest sequence identity to *Ca. Scalindua sorokini* (again 98% in both cases). Sequence identity to *Ca. Scalindua brodae* and *Ca. Scalindua* spp. sequences  
 400 detected previously in the Namibian OMZ (Kuypers et al., 2005) was 96%. Lowest sequence identity is seen with *Ca. Scalindua wagneri* (93%) and the Arabian Sea (94%). OTU-5 is placed outside of the BUS cluster (Fig. 6) and shows the highest sequence identity to Gulf of Mexico and Indian Ocean sediments (98% and 97% respectively). Sequence identity of OTU-5 in relation to the BUS OTU cluster is 94%.

## 405 4 Discussion

In the BUS, seasonal shifts in upwelling intensity create large spatiotemporal variability in oxygen concentrations (Bailey, 1991). Anammox has been reported previously in the low oxygen BUS water column (Kuypers et al. 2005), which therefore presents an ideal location to investigate anammox biomarkers. Here, we assess the distribution of BHT-*x* across the redox gradient in the BUS, to provide further insights into the application of BHT-*x* as a biomarker for *Ca. Scalindua* spp., and its  
 410 ratio over total BHT (BHT-*x* ratio) as a proxy for deoxygenation in dynamic upwelling systems.

### 4.1 Spatiotemporal distribution of anammox biomarkers along the redox gradient in the BUS

#### 4.1.1 Anammox constrained to the ODZ in the southern BUS shelf waters

During expeditions 64PE449 and 64PE450, the seasonal ODZ had developed in the southern BUS shelf waters (20°S–26°S) between ~50 mbss and the seafloor, with [O<sub>2</sub>] down to ~1.5–5.5 μmol L<sup>-1</sup>. Nutrient analyses revealed a large N deficit in the  
 415 ODZ (N deficit >10 μmol L<sup>-1</sup>; Fig. 7d; Table S2), suggesting major losses of bioavailable N by anammox and/or denitrification. Relatively high BHT-*x* abundances are detected at the southern shelf stations (St. 3–6, 10, 140) below 30 mbss (Fig. 3a). 16S rRNA gene analysis indeed indicated on-shelf presence of *Ca. Scalindua* spp. in the water masses below 30 mbss, with the highest abundance of *Ca. Scalindua* spp. 16S rRNA gene sequences relative to the total bacterial 16S rRNA gene sequence



pool below ~50 mbss (Fig. 3g). In addition to the *Ca. Scalindua* spp. 16S rRNA gene, ladderane IPLs are thought to reflect  
 420 living or recently

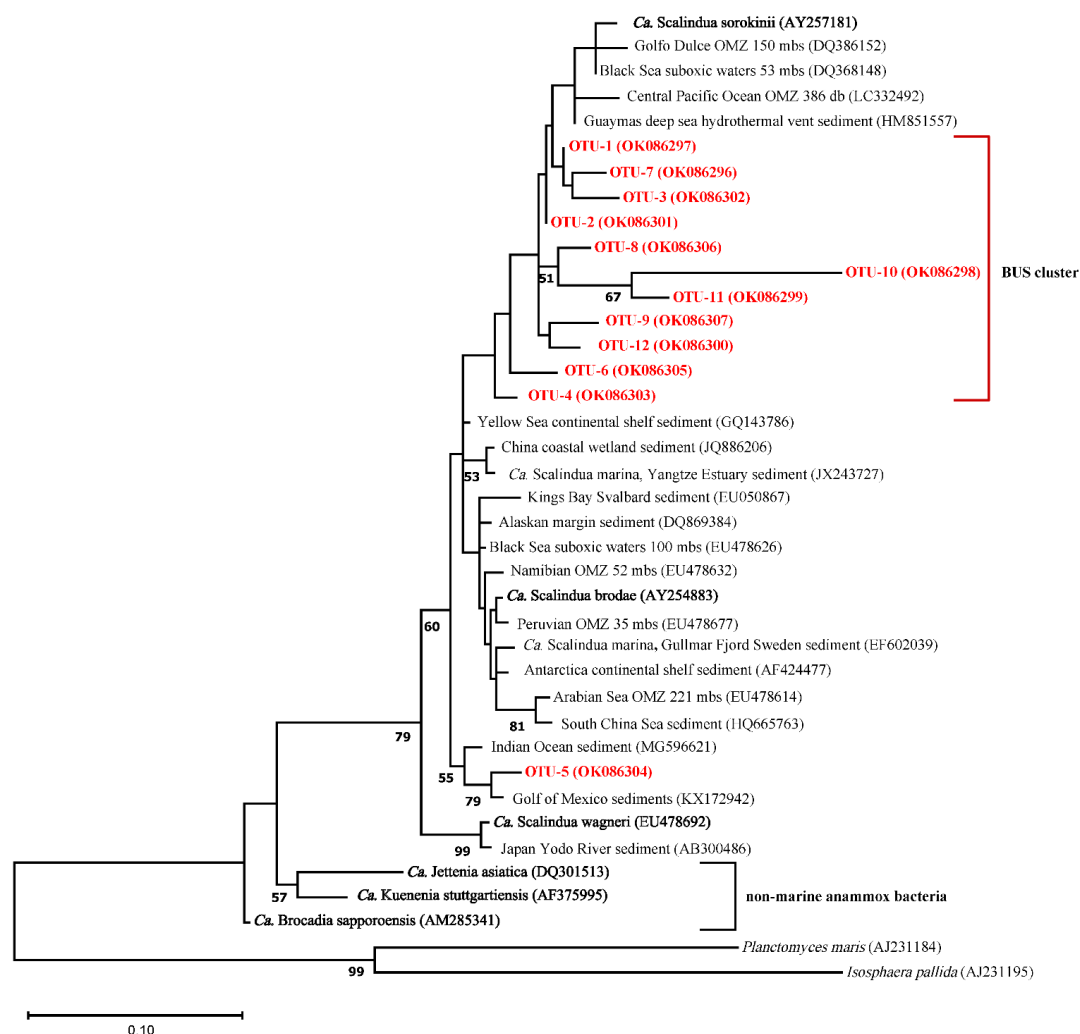


**Figure 6.** Maximum likelihood phylogenetic tree based on partial (422 bp) 16S rRNA gene sequences displaying the relationship of *Ca. Scalindua* spp. sequences of the 12 most abundant OTUs detected in the BUS (in red/bold; see Fig. S1 for relative abundance of each OTU) with other sequences from marine OMZs and sediments (in black), and anammox bioreactors (in black/bold). Bootstrap values higher than 50% are indicated in the nodes. The scale bar represents 10% estimated sequence divergence. The outgroup is formed by 16S rRNA gene sequences of *Planctomyces maris* and *Isosphaera pallida*. NCBI accession numbers are indicated in between parentheses.

dead anammox cells well (Harvey et al., 1986; Jaeschke et al., 2009a; Brandsma et al., 2011; Bale et al., 2014). Ladderane  
 IPLs are found on-shelf (St. 4, 5, 10, 117, and 140) between 30 mbss to the seafloor. The N deficit was significantly correlated  
 430 with both BHT-*x* and ladderane IPLs ( $r(60) = 0.53$ ,  $p = <0.001$ ; Table 2) and on-shelf N deficiencies were accompanied with  
 relatively high BHT-*x* and ladderane IPL abundances (Fig. 7). This suggests anammox was at least in part responsible for loss  
 of bioavailable N. In summary, the co-occurrence of BHT-*x* with *Ca. Scalindua* spp. 16S rRNA reads, ladderane IPLs and on-  
 shelf N deficiencies, indicate the presence of living (or recently dead) anammox cells in the BUS shelf waters (below ~30 to  
 50 mbss), consistent with earlier reports of anammox activity on the Namibian continental shelf waters (Kuyppers et al., 2005).



435 Additionally, *Ca. Scalindua* spp. 16S rRNA gene sequences and anammox biomarkers were detected in the more  
 oxygenated surface shelf waters (above 50 mbss), at ambient  $[O_2]$  up to  $\sim 45 \mu\text{mol L}^{-1}$  (and up to  $\sim 90 \mu\text{mol L}^{-1}$  in one case),  
 surpassing earlier established oxygen limits for anammox. Culturing studies have indicated that anammox bacteria are already  
 inhibited at  $[O_2]$  as low as  $1 \mu\text{mol L}^{-1}$  (Strous et al., 1997). In the environment, *Ca. Scalindua* spp. has been shown to remain  
 440 active at  $[O_2]$  up to  $9\text{--}20 \mu\text{mol L}^{-1}$  in the Namibian and Peruvian OMZs respectively (Kuypers et al., 2005; Hamersley et al.,  
 2007; Kalvelage et al., 2011) and up to  $\sim 9 \mu\text{mol L}^{-1}$  in the Black Sea (Jensen et al., 2008). A possible explanation has been  
 provided by Woebken et al. (2007), who showed that *Ca. Scalindua* spp. colonize microscopic particles in the BUS, which  
 provide suitable anaerobic micro-niches. Nevertheless, this was found to be restricted to ambient  $[O_2]$  levels below  $25 \mu\text{mol}$   
 $L^{-1}$ . Likely, our evidence for the presence of anammox bacteria in the more oxygenated BUS shelf waters reflects material  
 transported upwards from the deeper ODZ. Upwelled waters from the BC were clearly observed at stations south of the ABF  
 445 (St. 1–6, 10, 117 and 140;  $20^\circ\text{S}\text{--}26^\circ\text{S}$ ), as indicated by the relatively low SST and salinity at the halocline (Fig. 2c, d; S1).

**Table 2.** Pearson's correlation matrix between BHT-*x*, oxygen ( $O_2$ ), ammonium ( $NH_4^+$ ), nitrite ( $NO_2^-$ ), ladderane IPLs (IPLs), nitrogen  
 deficiency (N def), temperature (Temp), salinity (Sal) and BHT-*x*. *r*-values indicate Pearson's correlation coefficient. *p*-values indicate the  
 significance level (2-tailed) with bold numbers indicating that correlation is significant at the 0.05.

		BHT- <i>x</i>	IPLs	BHT- <i>x</i> ratio	$NO_2^-$	$NH_4^+$	N def.	Temp.	Sal.	$O_2$
<b>BHT-<i>x</i></b>	<i>r</i> -value	-	<b>0.65</b>	<b>0.59</b>	0.12	0.17	<b>0.53</b>	0.02	-0.01	-0.33
	<i>p</i> -value		<0.001	<0.001	0.36	0.19	<0.001	0.88	0.92	0.01
<b>IPLs</b>	<i>r</i> -value	<b>0.65</b>	-	<b>0.52</b>	-0.02	-0.03	<b>0.53</b>	0.09	0.08	<b>-0.29</b>
	<i>p</i> -value	<0.001		<0.001	0.88	0.83	<0.001	0.51	0.57	0.02
<b>BHT-<i>x</i> ratio</b>	<i>r</i> -value	<b>0.59</b>	<b>0.52</b>	-	-0.04	0.13	<b>0.63</b>	-0.04	-0.06	<b>-0.35</b>
	<i>p</i> -value	<0.001	<0.001		0.74	0.31	<0.001	0.76	0.66	0.01
<b><math>NO_2^-</math></b>	<i>r</i> -value	0.12	-0.02	-0.04	-	<b>0.62</b>	0.07	0.23	<b>0.3</b>	<b>-0.3</b>
	<i>p</i> -value	0.36	0.88	0.74		<0.001	0.61	0.08	0.02	0.02
<b><math>NH_4^+</math></b>	<i>r</i> -value	0.17	-0.03	0.13	<b>0.62</b>	-	<b>0.49</b>	0.17	0.17	<b>-0.32</b>
	<i>p</i> -value	0.19	0.83	0.31	<0.001		<0.001	0.20	0.19	0.01
<b>N def.</b>	<i>r</i> -value	<b>0.53</b>	<b>0.53</b>	<b>0.63</b>	0.07	<b>0.49</b>	-	0.04	-0.01	<b>-0.37</b>
	<i>p</i> -value	<0.001	<0.001	<0.001	0.61	<0.001		0.76	0.95	<0.005
<b>Temp.</b>	<i>r</i> -value	0.02	0.09	-0.04	0.23	0.17	0.04	-	<b>0.9</b>	-0.18
	<i>p</i> -value	0.88	0.512	0.759	0.076	0.197	0.757		<0.001	0.159
<b>Sal.</b>	<i>r</i> -value	-0.01	0.08	-0.06	<b>0.3</b>	0.17	-0.01	<b>0.9</b>	-	<b>-0.29</b>
	<i>p</i> -value	0.92	0.57	0.66	0.03	0.19	0.95	<0.001		0.02
<b><math>O_2</math></b>	<i>r</i> -value	<b>-0.33</b>	<b>-0.29</b>	<b>-0.35</b>	<b>-0.3</b>	<b>-0.32</b>	<b>-0.37</b>	-0.18	<b>-0.29</b>	-
	<i>p</i> -value	0.01	0.02	0.01	0.02	0.01	<0.005	0.17	0.02	

450

#### 4.1.2 Absence of anammox biomarkers near and north of the Angolan Benguela Front

Evidence for the presence of *Ca. Scalindua* spp., as indicated by 16S rRNA gene sequences, BHT-*x* and IPL ladderane  
 concentrations, was completely lacking at stations sampled north of the ABF (St. 8 and 55). At the time of sampling, large  
 horizontal gradients in SST and salinity existed around  $\sim 19.8^\circ\text{S}$ , fanning out seaward (Fig. 2c, d), indicating that the ABF had  
 455 developed at this latitude (Shannon et al., 1987; Loick et al., 2005). The ODZ did not extend past the frontal zone, and north  
 of the ABF, oxygen depletion occurred only down to  $\sim 20 \mu\text{mol L}^{-1}$  (between 150–500 mbss), which likely inhibited anammox  
 (Strous et al., 1997; Woebken et al. 2007; Kalvelage et al., 2011). At St. 117, located just south of ABF,  $[O_2]$  was below  $\sim 20$   
 $\mu\text{mol L}^{-1}$  at  $\sim 50$  mbss (down to  $\sim 3 \mu\text{mol L}^{-1}$  at 85 mbss; Fig. 3c), yet evidence of anammox was sparse. St. 117 was the only  
 BUS station where N was not limited (N deficit  $< 0 \mu\text{mol L}^{-1}$ ), revealing that loss of bioavailable nitrogen by anammox and/or  
 460 denitrification was absent or limited here (Fig 7h; Table S2). No BHT-*x* was detected, and only very low abundances of



ladderane IPLs ( $8.6 \times 10^4$  ru  $L^{-1}$ ; Table 2) and *Ca. Scalindua* spp. 16S rRNA gene sequences (0.001%; Fig. 3g) were detected at 85 mbss. Possibly, the water column at St. 117 had only recently become oxygen depleted. If so, the slow growth rate of anammox bacteria (e.g. Strous et al., 1999; Jetten et al., 2009) could explain why biomarker and 16S rRNA gene evidence for the presence of anammox bacteria was sparse at the time of sampling.

465 Salinity, temperature or nutrient ( $NO_2^-$  and  $NH_4^+$ ) concentrations were not seen to influence biomarker distributions in the BUS: i.e. no correlation was observed between these physiochemical parameters and BHT- $x$  or ladderane IPLs (Table 2). This agrees with earlier findings. *Ca. Scalindua* spp. have an optimal temperature range of 10–30 °C (Awata et al., 2012; Awata et al., 2013), well within the temperature range found in the BUS. Furthermore, changes in salinity have not been found to effect abundance of *Ca. Scalindua* spp. (Awata et al., 2012; Awata et al., 2013), and *Ca. Scalindua* spp. is known to have  
 470 an extremely low affinity for  $NO_2^-$  and  $NH_4^+$  (Awata et al., 2013). In our study, only  $[O_2]$  returned a weak but significant negative correlation with BHT- $x$  ( $r(60) = -0.33$ ,  $\rho = 0.01$ ) and ladderane IPLs ( $r(60) = -0.29$ ,  $\rho = 0.02$ ).

#### 4.1.3 Lateral transport of anammox biomarkers to oxygenated offshore waters

In the more oxygenated offshore waters (up to  $\sim 180 \mu\text{mol } L^{-1}$ ) BHT- $x$  was observed at St. 1, 2, 8 and 9, whereas ladderane IPLs were not detected and the relative abundance of the *Ca. Scalindua* spp. 16S rRNA gene was low (Fig. 3). The offshore N  
 475 deficit was limited ( $< 4 \mu\text{mol } L^{-1}$ ; Fig. 7d) and earlier reports (Kuypers et al., 2005) did not find anammox bacteria to be active in the BUS at an offshore station where bottom waters exceeded  $20 \mu\text{mol } L^{-1}$ . Yet, at St. 2, high concentration of ladderane FAs were observed alongside the presence of BHT- $x$  (Fig. 5a). To determine the provenance of ladderane FAs observed at St. 2, the  $NL_5$  index was used (Table S5). The  $NL_5$  index is correlated to the *in situ* growth temperature of anammox bacteria (Rattray et al. 2010). At St. 2,  $NL_5$  derived temperatures ( $21.0^\circ\text{C}$  at 250 mbss and  $15.6^\circ\text{C}$  at 710 mbss;) deviated strongly from  
 480 CTD measured temperatures ( $11.2$  and  $5.5^\circ\text{C}$ , respectively), indicating ladderane FAs had most likely been synthesised in warmer waters. In contrast, at the shelf stations 6 and 140,  $NL_5$  derived temperatures ( $7.4$ – $15.0^\circ\text{C}$ ; between 30–85 mbss) were close to CTD temperature measurements ( $12.5$ – $13.4^\circ\text{C}$ ; between 30–85 mbss), indicating *in situ* synthesis of the observed ladderane FAs. Likely, ladderane FAs detected at offshore St. 2 originated in, and were transported from, the warmer shelf waters.

485 Mollenhauer et al. (2007) showed that radiocarbon ages of lipid biomarkers in the BUS increased with distance from shore and water depth, as a consequence of lateral organic matter transport over the Namibian margin. In fact, most of the organic matter deposited offshore was found to derive from the shelf (Mollenhauer et al., 2007). Thus, lateral offshore transport of organic matter in the nepheloid layer of the water column taking place in the BUS (Mollenhauer et al., 2007), may have transported the ladderane FAs and BHT- $x$  from the ODZ on the shelf to offshore waters. Absence of evidence for living  
 490 anammox bacteria (e.g. 16S rRNA gene sequences and IPL lipids; Fig. 5a) at 125 and 250 mbss at St. 2 further strongly suggests an allochthonous origin of ladderane FAs and BHT- $x$ .

#### 4.1.4 Seasonality in anammox biomarker distributions

Large seasonal variations in water column oxygen concentration occur in the BUS. At the time of sampling, the Lüderitz upwelling cell was apparent at  $\sim 26^\circ\text{S}$ , appearing as a water mass with low SSTs, low salinities (Fig. 2c, d), and high chlorophyll  
 495  $\alpha$  concentrations (Table S1). Here, the water column was sampled once in February (St. 6) and once in March (St. 140) to explore the occurrence and distribution of anammox lipid biomarkers and 16S rRNA gene sequences, as the ODZ developed on the continental shelf (sediment depth 100 mbss).

In February (Fig. 5b), the nutrient, oxygen and temperature profiles show a highly stratified water column. A strong oxycline is present around  $\sim 20$  mbss, with near anoxic conditions in the bottom waters (down to  $\sim 3 \mu\text{mol } L^{-1}$ ). 16S rRNA  
 500 amplicon sequences of *Ca. Scalindua* spp. and BHT- $x$  were detected below 40 mbss and 50 mbss, respectively, with (relative) abundances increasing with depth. Ladderane FAs followed a similar distribution, increasing in concentration with water



column depth. However, ladderane IPLs were not detected throughout the water column, which may indicate that anammox bacteria were not yet a dominant feature in the water column community. The accumulation of ammonium in the bottom waters, corresponding to a very high N deficit of  $38 \mu\text{mol L}^{-1}$  (Table S2), would suggest that denitrification was much more active than anammox (Richards et al., 1965).

In March (Fig. 5c), the same location showed distinct differences in physiochemical properties. SST was  $\sim 1.5^\circ\text{C}$  lower, inducing water column mixing, leading to weakened stratification. This is consistent with earlier reported seasonality, as lower temperatures and increased upwelling commence in austral autumn, resulting in decreased SSTs (Monteiro et al., 2008; Louw et al., 2016).  $[\text{O}_2]$  at the surface ( $<10$  mbss) was much lower ( $\sim 137 \mu\text{mol L}^{-1}$ ) than observed in February ( $\sim 204 \mu\text{mol L}^{-1}$ ) and the oxycline was less developed. The nutrient-rich sub-thermocline waters probably mixed with the surface waters, resulting in similar  $\text{NO}_2^-$ ,  $\text{NO}_3^-$ , and  $\text{NH}_4^+$  concentrations throughout the water column. Salinity was relatively high (35.2–36.2 psu), indicating the late summer (Feb–April) salinity maximum ( $S > 35.1$  psu; corresponding to the oxygen minimum) had set in (Monteiro et al., 2008). *Ca. Scalindua* spp. 16S rRNA genes were detected at all sampled depths, including 10 mbss. Ladderane IPLs were present in relatively high abundance throughout the water column at all sampled depths (35–85 mbss). Likewise, BHT-*x* and ladderane FA were also observed at all sampled depths. The ladderane FA and BHT-*x* concentrations were slightly lower than observed in February at 85 mbss, which may indicate that particulate material sank to the sea-floor, was degraded, or was transported elsewhere before the water column was sampled again in March.

Our findings suggest a strong temporal variability in the presence of anammox bacteria and their synthesized lipids at  $26^\circ\text{S}$ , corresponding to a large shift in hydrographic characteristics of the water column. In all likelihood, anammox bacteria only became an established community at the end of austral summer, once the oxygen minimum had set in.

#### 4.2 Application and constraints on the use of BHT-*x* as a biomarker for *Ca. Scalindua*

In the BUS, sequences taxonomically assigned to *Ca. Scalindua* spp. were detected at 11 out of 13 stations (Fig. 3g, n). A phylogenetically closely related cluster of *Ca. Scalindua* OTUs could be identified (i.e. the BUS OTU cluster indicated in Fig. 6). The BUS OTU cluster displayed a large sequence identity to *Ca. Scalindua sorokinii* isolated from the Guaymas deep sea hydrothermal vents and the Black Sea suboxic waters (98%; Table S7) and *Ca. Scalindua brodae* (97%; Table S7). BHT-*x* has been shown to be uniquely synthesized by marine anammox, using *Ca. S. brodae* enrichment cultures (Rush et al., 2014; Schwartz-Narbonne et al., 2020). In accordance with these reports, BHT-*x* was observed at the same 11 stations where *Ca. Scalindua* 16S rRNA gene sequences were detected.

At shelf stations (St. 3–6, 10, 18, 55, 117, 140), the presence of BHT-*x* co-occurred with the detection of *Ca. Scalindua* spp. 16S rRNA gene sequences at all depths except St. 5, 30 mbss. A multivariate binomial regression was performed to determine if the relative abundance of BHT-*x* can be used to predict the likelihood of 16S rRNA *Ca. Scalindua* spp. sequence presence in the BUS. This test showed that the presence of BHT-*x* significantly predicts the presence of *Ca. Scalindua* spp. in 78.8% of all cases ( $p < 0.001$ ), showing BHT-*x* is a suitable biomarker for *Ca. Scalindua* spp. even in complex upwelling regions such as the BUS. However, in the BUS, *Ca. Scalindua* spp. 16S rRNA gene sequences constituted only a small portion of the total bacterial pool (max. 2.7‰; Fig. 3g). Low abundance of marine anammox bacteria in comparison to other phylogenetic groups in marine ecosystems has been reported previously (Woebken et al., 2007) and is likely caused by slow cell division rates (Strous et al., 1999; Jetten et al., 2009). Even so, it cannot be excluded that well-known PCR biases might also have led to a low coverage of *Ca. Scalindua* spp. reads (e.g. Pinto & Raskin, 2012).

*Ca. Scalindua* spp. 16S rRNA gene sequences were also detected in offshore waters. Yet, co-occurrence with BHT-*x* was limited (only in four of the 19 offshore SPM samples) and the extremely low relative abundance of *Ca. Scalindua* spp. 16S rRNA gene sequences here (0–0.4‰; Fig. 3n) and BHT-*x* concentrations (factor 10 to 100 lower than at shelf stations) make it unlikely that anammox bacteria formed an active community. Rather, lateral organic matter transport, discussed in



section 4.1.3, seems to contribute to the BHT-*x* concentrations observed offshore. Considerations must thus be taken when interpreting low abundances of BHT-*x*, as these may inaccurately suggest the presence of living *Ca. Scalindua*.

545

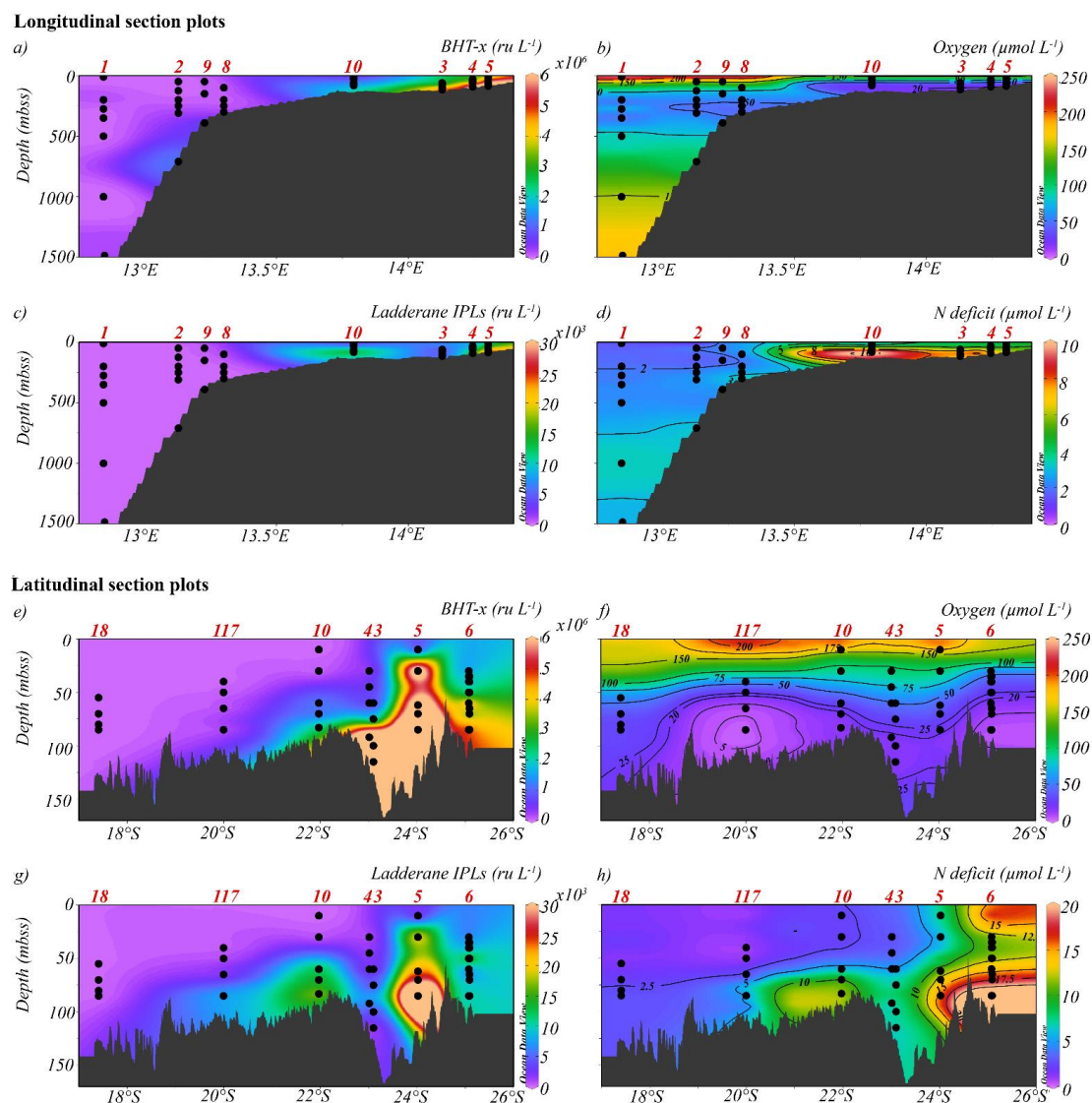


**Figure 7.** Longitudinal (a-d) and latitudinal (e-h) section plots showing interpolated concentrations of dissolved oxygen (a,e), nitrogen deficit (b,g), BHT-*x* (c,f) and ladderane IPLs (d,h). Contour lines for O<sub>2</sub> and N deficit concentrations are added to their plots.

### 4.3 Application and constraints on the use of BHT-*x* ratio as a biomarker for low oxygen conditions

550 In addition to being a useful biomarker for *Ca. Scalindua*, BHT-*x* has been applied as a proxy for low oxygen concentration in marine systems. Saénz et al (2011) proposed the ratio of BHT-*x* over total BHT as a proxy for suboxic-anoxic conditions (defined as [O<sub>2</sub>] < 5  $\mu\text{mol L}^{-1}$ ), since BHT-*x* was only found in low-oxygen settings, whereas BHT is ubiquitously synthesized by mostly aerobic bacteria. The discovery that BHT-*x* is uniquely synthesized by marine anammox (Rush et al., 2014; Schwarz-Narbonne et al., 2019) provided further evidence for this application of the BHT-*x* ratio, as it reflects the contribution of BHT-*x* synthesised by the anaerobic '*Ca. Scalindua* spp.' to the total BHT pool. In the water columns of the Arabian Sea, Peru Margin and Cariaco Basin, Saénz et al. (2011) found that when [O<sub>2</sub>] was > 50  $\mu\text{mol kg}^{-1}$  (~50  $\mu\text{mol L}^{-1}$ ), the BHT-*x* ratio



remained below 0.03 (with one exception). Similarly, at BUS shelf stations, when  $[O_2]$  was  $>50 \mu\text{mol L}^{-1}$ , the BHT- $x$  ratio remained below 0.04, in all but one case (St. 5 at 30 mbss). However, at five offshore sites where  $[O_2]$  was  $>50 \mu\text{mol L}^{-1}$  (up to  $\sim 180 \mu\text{mol L}^{-1}$ ), BHT- $x$  ratios  $>0.04$  were observed. The BHT- $x$  concentrations were markedly lower at these offshore stations than at shelf stations, yet the equally low BHT concentrations (Table S3) resulted in relatively high BHT- $x$  ratios. To circumvent false interpretation of the ratio due to low BHT abundances or allochthonous BHT- $x$  material (considering offshore BHT- $x$  likely derived from the on-shelf ODZ), we suggest using a higher threshold as a proxy for low oxygen conditions in systems with known lateral transport of organic matter. At both offshore and on-shelf sites, when  $[O_2]$  was  $>50 \mu\text{mol L}^{-1}$ , the BHT- $x$  ratio remained below 0.18, in all but one case (St. 5 at 30 mbss), which may thus act as a safer threshold to infer deoxygenation. In addition, a ratio of  $>0.18$  corresponded in all cases (except one) with the presence of the *Ca. Scalindua* spp. 16S rRNA gene, which was not the case for ratios  $>0.04$ .

As *Ca. Scalindua* spp. synthesizes both BHT and BHT- $x$ , the BHT- $x$  ratio was also calculated in a *Ca. S. brodae* biomass enrichment, where it was found to be 0.38. In the BUS, on-shelf stations had an average BHT- $x$  ratio of  $0.21 \pm 0.13$ , indicating that *Ca. Scalindua* spp. likely contributed to most of the BHT at these sites. In addition, three shelf sites (St. 4 at 92 mbss, St. 140 at 40 and 50 mbss; Fig. 4) surpassed a ratio of 0.38. This indicates the BUS OTUs taxonomically assigned to *Ca. Scalindua* spp. (Fig. 6) synthesized BHT- $x$  in a higher fractional abundance than observed in the *Ca. Scalindua* enrichment. Possibly, *Ca. Scalindua* sp. phylogeny of the BUS OTUs and/or environmental conditions may influence the relative concentrations at which BHT- $x$  and BHT are synthesized. This may also explain differences in the observed fractional abundance of BHT- $x$  in *Ca. S. brodae* enrichments between this study and earlier reports (Rush et al., 2014; Schwartz-Narbonne et al., 2019), considering the lipid extraction methods and analytical techniques used were similar.

## 5 Conclusion

This study reveals a strong spatiotemporal variability in the presence of anammox bacteria (as reflected by their 16S rRNA gene sequences) and their membrane lipids in the Benguela Upwelling System (BUS), which corresponds to differences in hydrographic characteristics of the water column. By elucidating the distribution of BHT- $x$  across a large oxygen gradient, and comparing it to distributions of ladderane IPLs, ladderane FAs and *Ca. Scalindua* spp. 16S rRNA gene sequences, we assessed the suitability of BHT- $x$  as a lipid biomarker for *Ca. Scalindua* spp., as well as its ratio over total BHT as a proxy for anoxia. On the continental shelf, BHT- $x$  co-occurred with the detection of *Ca. Scalindua* spp. 16S rRNA genes in all but one cases, further highlighting its suitability as a lipid biomarker for marine anammox in the sedimentary record of upwelling regions. The southernmost shelf station ( $\sim 25^\circ\text{S}$ ) was sampled 27 days apart and showed that anammox bacteria only became an established community in the shelf waters at the end of austral summer. At the offshore stations, ladderane FAs and low concentrations of BHT- $x$  were also observed to accumulate in relatively oxygenated waters ( $[O_2]$  up to  $\sim 180 \mu\text{mol L}^{-1}$ ), while ladderane IPLs were constrained to the shelf stations. Calculating the  $NL_5$  index for ladderane FAs indicated that offshore ladderane FAs were not synthesized *in situ* and likely originated from the shelf. This must be taken into consideration when using BHT- $x$  and ladderane FAs as lipid biomarkers for *in situ* water column anammox. Lastly, at shelf stations, where  $[O_2]$  was  $>50 \mu\text{mol L}^{-1}$ , the BHT- $x$  ratio remained below 0.04, in all but one case. Yet, laterally transported BHT- $x$  resulted in high offshore BHT- $x$  ratio values ( $>0.04$ ) in oxygenated waters. We therefore suggest to use a BHT- $x$  ratio threshold of 0.18 to infer low oxygen conditions in sedimentary records of dynamic upwelling systems: throughout the BUS, when  $[O_2]$  was  $>50 \mu\text{mol L}^{-1}$ , the BHT- $x$  ratio remained below 0.18 (in all but one case).



595 *Data availability.* This data will be deposited within the open-access library PANGAEA (doi to be delivered later). Unassembled sequences are submitted to NCBI under BioProject number PRJNA761075. Individual sequences of OTUs 1-12 are published in GenBank under accession numbers OK086296 – OK086307.

*Supplement.* The supplement related to this article will be made available online (doi to be delivered later).

*Acknowledgements.* This research is supported by the Soehngen Institute of Anaerobic Microbiology (SIAM) Gravitation Grant (024.002.002) of the Netherlands Ministry of Education, Culture and Science (OCW) and the Netherlands Organization  
 600 for Scientific Research (NWO) to J.S.S.D. and L.V. We kindly thank the captain and crew of the R/V *Pelagia* and the co-chief scientist on board, Dr. Zeynep Erdem, for facilitating the collection of all sampled material. Olga Żygadłowska is thanked for helping with the on-board sample processing and her great enthusiasm in doing so. We further greatly appreciate the help of Dr. Nicole Bale, with her knowledge on Bligh & Dyer extractions. Marianne Baas is thanked for deploying the *in situ* pumps during the second expedition. In addition, we thank Karel Bakker and Jan van Ooijen for the onboard NUTS analyses. We are  
 605 also grateful for the support Denise Dorhout and Monique Verweij have delivered in the lipid lab and Maartje Brouwer and Sanne Vreugdenhil in the molecular labs. Lastly, Tom Vaessen is thanked for taking the time to discuss statistics.

*Author contribution.* ZRvK wrote the manuscript; PK and DR were in charge of the research expeditions; ZRvK, DR and PK performed the sample collection; ZRvK performed the laboratory work and data analysis. LV and HJW contributed to the data  
 610 analysis of the 16S rRNA gene sequences; ECH optimized UHPLC measurements. ECH and DR contributed to the lipid data analysis. DR, JSSD, LV and ZRvK designed and conceptualized the project; All co-authors provided critical feedback and helped shape the research, analysis and manuscript.

*Competing interests.*

615 The authors declare that they have no conflict of interest.

## References

1. Awata, T., Oshiki, M., Kindaichi, T., Ozaki, N., Ohashi, A. and Okabe, S.: Physiological characterization of an anaerobic ammonium-oxidizing bacterium belonging to the “Candidatus *Ca. Scalindua*” group, Appl. Environ. Microbiol., 79(13), 4145–4148, doi:10.1128/AEM.00056-13, 2013.
- 620 2. Awata, T., Tanabe, K., Kindaichi, T., Ozaki, N. and Ohashi, A.: Influence of temperature and salinity on microbial structure of marine anammox bacteria, Water Sci. Technol., 66(5), 958–964, doi:10.2166/wStation2012.234, 2012.
3. Bailey, G. W.: Organic carbon flux and development of oxygen deficiency on the modern Benguela continental shelf south of 22°S: Spatial and temporal variability, Geol. Soc. Spec. Publ., 58(58), 171–183, doi:10.1144/GSL.SP.1991.058.01.12, 1991.
- 625 4. Bale, N. J., Villanueva, L., Fan, H., Stal, L. J., Hopmans, E. C., Schouten, S. and Sinninghe Damsté, J. S.: Occurrence and activity of anammox bacteria in surface sediments of the southern North Sea, FEMS Microbiol. Ecol., 89(1), 99–110, doi:10.1111/1574-6941.12338, 2014.
5. Bale, N. J., Ding, S., Hopmans, E. C., Arts, M. G. I., Villanueva, L., Boschman, C., Haas, A. F., Schouten, S. and Sinninghe Damsté, J. S.: Lipidomics of Environmental Microbial Communities. I: Visualization of  
 630 Component Distributions Using Untargeted Analysis of High-Resolution Mass Spectrometry Data, Front. Microbiol., 12, doi: 10.3389/fmicb.2021.659302, 2021



- 635 6. Berndmeyer, C., Thiel, V., Schmale, O., Wasmund, N. and Blumenberg, M.: Biomarkers in the stratified water column of the Landsort Deep (Baltic Sea), *Biogeosciences*, 11(23), 7009–7023, doi:10.5194/bg-11-7009-2014, 2014.
7. Boumann, H. A., Hopmans, E. C., Van De Leemput, I., Op Den Camp, H. J. M., Van De Vossenberg, J., Strous, M., Jetten, M. S. M., Sinninghe Damsté, J. S. and Schouten, S.: Ladderane phospholipids in anammox bacteria comprise phosphocholine and phosphoethanolamine headgroups, *FEMS Microbiol. Lett.*, 258(2), 297–304, doi:10.1111/j.1574-6968.2006.00233.x, 2006.
- 640 8. Boyer, D., Cole, J. and Bartholomae, C.: Southwestern Africa: Northern Benguela Current region, *Mar. Pollut. Bull.*, 41, 123–140, 2000.
9. Brandsma, J., van de Vossenberg, J., Risgaard-Petersen, N., Schmid, M. C., Engström, P., Eurenus, K., Hulth, S., Jaeschke, A., Abbas, B., Hopmans, E. C., Strous, M., Schouten, S., Jetten, M. S. M. and Damsté, J. S. S.: A multi-proxy study of anaerobic ammonium oxidation in marine sediments of the Gullmar Fjord, Sweden, *Environ. Microbiol. Rep.*, 3(3), 360–366, doi:10.1111/j.1758-2229.2010.00233.x, 2011.
- 645 10. Breitburg, D., Levin, L. A., Oschlies, A., Grégoire, M., Chavez, F. P., Conley, D. J., Garçon, V., Gilbert, D., Gutiérrez, D., Isensee, K., Jacinto, G. S., Limburg, K. E., Montes, I., Naqvi, S. W. A., Pitcher, G. C., Rabalais, N. N., Roman, M. R., Rose, K. A., Seibel, B. A., Telszewski, M., Yasuhara, M. and Zhang, J.: Declining oxygen in the global ocean and coastal waters, *Science* (80-. ), 359(6371), doi:10.1126/science.aam7240, 2018.
- 650 11. Brüchert, V., Currie, B., Peard, K. R., Lass, U., Endler, R., Dübecke, A., Julies, E., Leipe, T. and Zitzmann, S.: Biogeochemical and Physical Control on Shelf Anoxia and Water Column Hydrogen Sulphide in the Benguela Coastal Upwelling System Off Namibia., 2006.
12. Chapman, P. and Shannon, L. V.: Seasonality in the oxygen minimum layers at the extremities of the Benguela system, *South African J. Mar. Sci.*, 5(1), 85–94, doi:10.2989/025776187784522162, 1987.
- 655 13. Codispoti, L. A., Brandes, J. A., Christensen, J. P., Devol, A. H., Naqvi, S. W. A., Paerl, H. W. and Yoshinari, T.: The oceanic fixed nitrogen and nitrous oxide budgets: Moving targets as we enter the Anthropocene? *Sci. Mar.*, 65(2), 85–105, doi:10.3989/scimar.2001.65s285, 2001.
14. Ekau, W. and Verheye, H. M.: Influence of oceanographic fronts and low oxygen on the distribution of ichthyoplankton in the Benguela and southern Angola currents, *African J. Mar. Sci.*, 27(3), 629–639, doi:10.2989/18142320509504123, 2005.
- 660 15. Gruber, N.: The Ocean Carbon Cycle and Climate., doi:10.1007/978-1-4020-2087-22004, 2004.
16. Hamersley, M. R., Lavik, G., Woecklen, D., Rattray, J. E., Lam, P., Hopmans, E. C., Sinninghe Damsté, J. S., Krüger, S., Graco, M., Gutiérrez, D. and Kuypers, M. M. M.: Anaerobic ammonium oxidation in the Peruvian oxygen minimum zone, *Limnol. Oceanogr.*, 52(3), 923–933, doi:10.4319/lo.2007.52.3.0923, 2007.
- 665 17. Harvey, H. R., Fallon, R. D. and Patton, J. S.: The effect of organic matter and oxygen on the degradation of bacterial membrane lipids in marine sediments, *Geochim. Cosmochim. Acta*, 50(5), 795–804, doi:10.1016/0016-7037(86)90355-8, 1986.
18. Jaeschke, A., Rooks, C., Trimmer, M., Nicholls, J. C., Hopmans, E. C., Schouten, S. and Sinninghe Damsté, J. S.: Comparison of ladderane phospholipids and core lipids as indicators for anaerobic ammonium oxidation (anammox) in marine sediments, *Geochim. Cosmochim. Acta*, 73, 2077–2088, doi: doi:10.1016/j.gca.2009.01.013, 2009a.
- 670 19. Jaeschke, A., Ziegler, M., Hopmans, E. C., Reichart, G. J., Lourens, L. J. and Schouten, S.: Molecular fossil evidence for anaerobic ammonium oxidation in the Arabian Sea over the last glacial cycle, *Paleoceanography*, 24(2), 1–11, doi:10.1029/2008PA001712, 2009b.
- 675



20. Jaeschke, A., Abbas, B., Zabel, M., Hopmans, E. C., Schouten, S. and Sinninghe Damsté, J. S.: Molecular evidence for anaerobic ammonium-oxidizing (anammox) bacteria in continental shelf and slope sediments off northwest Africa, *Limnol. Oceanogr.*, 55(1), 365–376, doi:10.4319/lo.2010.55.1.0365, 2010.
- 680 21. Jensen, M. M., Kuypers, M. M. M., Lavik, G. and Thamdrup, B.: Rates and regulation of anaerobic ammonium oxidation and denitrification in the Black Sea, *Limnol. Oceanogr.*, 53(1), 23–36, doi:10.4319/lo.2008.53.1.0023, 2008.
22. Jetten, M.S.M., van Niftrik, L., Strous, M., Kartal, B., Kjeltens, J.T. and op den Camp, H.J.: Biochemistry and molecular biology of anammox bacteria, *Crit. Rev. Biochem.*, 44, 65–84, doi: 10.1109/cleoe-qec.2009.5193615, 2009.
- 685 23. Kalvelage, T., Jensen, M. M., Contreras, S., Revsbech, N. P., Lam, P., Günter, M., LaRoche, J., Lavik, G. and Kuypers, M. M. M.: Oxygen sensitivity of anammox and coupled N-cycle processes in oxygen minimum zones, *PLoS One*, 6(12), doi:10.1371/journal.pone.0029299, 2011.
24. Kuypers, M. M. M., Silekers, A. O., Lavik, G., Schmid, M., Jørgensen, B. B., Kuenen, J. G., Sinninghe Damsté, J. S., Strous, M. and Jetten, M. S. M.: Anaerobic ammonium oxidation by anammox bacteria in the Black Sea, *Nature*, 422(6932), 608–611, doi:10.1038/nature01472, 2003.
- 690 25. Kuypers, M. M. M., Lavik, G., Woebken, D., Schmid, M., Fuchs, B. M., Amann, R., Jørgensen, B. B. and Jetten, M. S. M.: Massive nitrogen loss from the Benguela upwelling system through anaerobic ammonium oxidation, *Proc. Natl. Acad. Sci. U. S. A.*, 102(18), 6478–6483, doi:10.1073/pnas.0502088102, 2005.
26. Lam, P., Lavik, G., Jensen, M. M., Van Vossenberg, J. De, Schmid, M., Woebken, D., Gutiérrez, D., Amann, R., Jetten, M. S. M. and Kuypers, M. M. M.: Revising the nitrogen cycle in the Peruvian oxygen minimum zone, *Proc. Natl. Acad. Sci. U. S. A.*, 106(12), 4752–4757, doi:10.1073/pnas.0812444106, 2009.
- 695 27. Louw, D. C., van der Plas, A. K., Mohrholz, V., Wasmund, N., Junker, T. and Eggert, A.: Seasonal and interannual phytoplankton dynamics and forcing mechanisms in the Northern Benguela upwelling system, *J. Mar. SyStation*, 157, 124–134, doi:10.1016/j.jmarsys.2016.01.009, 2016.
- 700 28. Mercier, H., Arhan, M. and Lutjeharms, J. R. E.: Upper-layer circulation in the eastern Equatorial and South Atlantic Ocean in January–March 1995, *Deep. Res. Part I Oceanogr. Res. Pap.*, 50(7), 863–887, doi:10.1016/S0967-0637(03)00071-2, 2003.
29. Mohrholz, V., Bartholomae, C. H., van der Plas, A. K. and Lass, H. U.: The seasonal variability of the northern Benguela undercurrent and its relation to the oxygen budget on the shelf, *Cont. Shelf Res.*, 28(3), 424–441, doi:10.1016/j.csr.2007.10.001, 2008.
- 705 30. Mollenhauer, G., Inthorn, M., Vogt, T., Zabel, M., Sinninghe Damsté, J. S. and Eglinton, T. I.: Aging of marine organic matter during cross-shelf lateral transport in the Benguela upwelling system revealed by compound-specific radiocarbon dating, *Geochemistry, Geophys. Geosystems*, 8(9), doi:10.1029/2007GC001603, 2007.
- 710 31. Monteiro, F. M., Pancost, R. D., Ridgwell, A. and Donnadieu, Y.: Nutrients as the dominant control on the spread of anoxia and euxinia across the Cenomanian–Turonian oceanic anoxic event (OAE2): Model-data comparison, *Paleoceanography*, 27(4), 1–17, doi:10.1029/2012PA002351, 2012.
32. Oschlies, A., Brandt, P., Stramma, L. and Schmidtko, S.: Drivers and mechanisms of ocean deoxygenation, *Nat. Geosci.*, 11(7), 467–473, doi:10.1038/s41561-018-0152-2, 2018.
- 715 33. Ourisson, G. and Albrecht, P.: Geohopanoids: The Most Abundant Natural Products on Earth?, *Acc. Chem. Res.*, 25, 398–402, doi: 10.1021/ar00021a003, 1992.
34. Parada, A.E., Needham, D.M. and Fuhrman, J.A., Primers for marine microbiome studies. *Environ Microbiol.*, 18: 1403–1414. Doi: https://doi.org/10.1111/1462-2920.13023, 2016.



- 720 35. Paulmier, A. and Ruiz-Pino, D.: Oxygen minimum zones (OMZs) in the modern ocean, *Prog. Oceanogr.*, 80(3–4), 113–128, doi:10.1016/j.pocean.2008.08.001, 2009.
36. Pinto, A.J. & Raskin, L.: PCR Biases Distort Bacterial and Archaeal Community Structure in Pyrosequencing Datasets, *PLOS ONE*, 7(8), e4309, doi: 10.1371/journal.pone.0043093, 2012.
- 725 37. Pitcher, A., Villanueva, L., Hopmans, E. C., Schouten, S., Reichart, G. J. and Sinninghe Damsté, J. S.: Niche segregation of ammonia-oxidizing archaea and anammox bacteria in the Arabian Sea oxygen minimum zone, *ISME J.*, 5(12), 1896–1904, doi:10.1038/ismej.2011.60, 2011.
38. Rattray, J. E., Van De Vossenberg, J., Hopmans, E. C., Kartal, B., Van Niftrik, L., Rijpstra, W. I. C., Strous, M., Jetten, M. S. M., Schouten, S. and Damsté, J. S. S.: Ladderane lipid distribution in four genera of anammox bacteria, *Arch. Microbiol.*, 190(1), 51–66, doi:10.1007/s00203-008-0364-8, 2008.
- 730 39. Rattray, J. E., Van Vossenberg, J. De, Jaeschke, A., Hopmans, E. C., Wakeham, S. G., Lavik, G., Kuypers, M. M. M., Strous, M., Jetten, M. S. M., Schouten, S. and Sinninghe Damsté, J. S.: Impact of temperature on ladderane lipid distribution in anammox bacteria, *Appl. Environ. Microbiol.*, 76(5), 1596–1603, doi:10.1128/AEM.01796-09, 2010.
40. Redfield, A. C., Ketchum, B. H. and Richards, F. A.: The influence of organisms on the composition of sea water, in *The Sea*, vol. 2, edited by M. N. Hill, pp. 26–77, Interscience Publishers, New York, New York., 1963.
- 735 41. Richards, F. A., Cline, J. D., Broenkow, W. W. and Atkinson, L. P.: Some consequences of the decomposition of Organic Matter in Lake Nitinat, an anoxic fjord, *Limnol. Oceanogr.*, 10, 185–201, 1965.
42. Rush, D., Jaeschke, A., Hopmans, E. C., Geenevasen, J. A. J., Schouten, S. and Sinninghe Damsté, J. S.: Short chain ladderanes: Oxidic biodegradation products of anammox lipids, *Geochim. Cosmochim. Acta*, 75(6), 1662–1671, doi:10.1016/j.gca.2011.01.013, 2011.
- 740 43. Rush, D., Sinninghe Damsté, J. S., Poulton, S. W., Thamdrup, B., Garside, A. L., Acuña González, J., Schouten, S., Jetten, M. S. M. and Talbot, H. M.: Anaerobic ammonium-oxidising bacteria: A biological source of the bacteriohopanetetrol stereoisomer in marine sediments, *Geochim. Cosmochim. Acta*, 140, 50–64, doi:10.1016/j.gca.2014.05.014, 2014.
- 745 44. Rush, D., Talbot, H. M., Van Der Meer, M. T. J., Hopmans, E. C., Douglas, B. and Sinninghe Damsté, J. S.: Biomarker evidence for the occurrence of anaerobic ammonium oxidation in the eastern Mediterranean Sea during Quaternary and Pliocene sapropel formation, *Biogeosciences*, 16(12), 2467–2479, doi:10.5194/bg-16-2467-2019, 2019.
- 750 45. Sáenz, J. P., Wakeham, S. G., Eglinton, T. I. and Summons, R. E.: New constraints on the provenance of hopanoids in the marine geologic record: Bacteriohopanepolyols in marine suboxic and anoxic environments, *Org. Geochem.*, 42(11), 1351–1362, doi:10.1016/j.orggeochem.2011.08.016, 2011.
46. Sarmiento, J. L. and Gruber, N.: Global patterns of marine nitrogen fixation and denitrification, *Glob. biogeochemical cycles*, 11(2), 235–266, 1997.
- 755 47. Schmid, M. C., Risgaard-Petersen, N., Van De Vossenberg, J., Kuypers, M. M. M., Lavik, G., Petersen, J., Hulth, S., Thamdrup, B., Canfield, D., Dalsgaard, T., Rysgaard, S., Sejr, M. K., Strous, M., Op Den Camp, H. J. M. and Jetten, M. S. M.: Anaerobic ammonium-oxidizing bacteria in marine environments: Widespread occurrence but low diversity, *Environ. Microbiol.*, 9(6), 1476–1484, doi:10.1111/j.1462-2920.2007.01266.x, 2007.
- 760 48. Schmid, M., Walsh, K., Webb, R., Rijpstra, W. I. C., Van De Pas-Schoonen, K., Verbruggen, M. J., Hill, T., Moffett, B., Fuerst, J., Schouten, S., Damsté, J. S. S., Harris, J., Shaw, P., Jetten, M. and Strous, M.: Candidatus “*Ca. Scalindua brodae*”, sp. nov., Candidatus “*Ca. Scalindua wagneri*”, sp. nov., Two New



- Species of Anaerobic Ammonium Oxidizing Bacteria, *Syst. Appl. Microbiol.*, 26(4), 529–538, doi:10.1078/072320203770865837, 2003.
49. Schouten, S., Middelburg, J. J., Hopmans, E. C. and Sinninghe Damsté, J. S.: Fossilization and degradation  
 of intact polar lipids in deep subsurface sediments: A theoretical approach, *Geochim. Cosmochim. Acta*,  
 74(13), 3806–3814, doi:10.1016/j.gca.2010.03.029, 2010.
50. Schwartz-Narbonne, R., Schaeffer, P., Hopmans, E. C., Schenese, M., Charlton, E. A., Jones, D. M.,  
 Sinninghe Damsté, J. S., Farhan Ul Haque, M., Jetten, M. S. M., Lenggler, S. K., Murrell, J. C., Normand,  
 P., Nuijten, G. H. L., Talbot, H. M. and Rush, D.: A unique bacteriohopanetetrol stereoisomer of marine  
 anammox, *Org. Geochem.*, 143, doi:10.1016/j.orggeochem.2020.103994, 2020. Sinninghe Damsté, J. S.,  
 Rijpstra, W. I. C., Geenevasen, J. A. J., Strous, M. and Jetten, M. S. M.: Structural identification of ladderane  
 and other membrane lipids of planctomycetes capable of anaerobic ammonium oxidation (anammox), *FEBS  
 J.*, 272(16), 4270–4283, doi:10.1111/j.1742-4658.2005.04842.x, 2005.
51. Sinninghe Damsté, J. S., Strous, M., Rijpstra, W. I. C., Hopmans, E. C., Geenevasen, J. A. J., Van Duin, A.  
 C. T., Van Niftrik, L. A. and Jetten, M. S. M.: Linearly concatenated cyclobutane lipids form a dense  
 bacterial membrane, *Nature*, 419(6908), 708–712, doi:10.1038/nature01128, 2002.
52. Strous, M., van Gerven, E., Kuenen, J. G. and Jetten, M. S. M.: Effects of aerobic and microaerobic conditions  
 on anaerobic ammonium-oxidizing (anammox) sludge, *Appl. Environ. Microbiol.*, 63(6), 2446–2448, doi:  
 10.1128/aem.63.6.2446-2448.1997, 1997.
53. Strous, M., Fuerst, J. A., Kramer, E. H. M., Logemann, S., Muyzer, G., van de Pas-Schoonen, K. T., Webb,  
 R., Kuenen, J. G., Jetten, M. S. M.: Missing lithotroph identified as new planctomycete, *Nature*, 400(July),  
 1999.
54. Sturt, H. F., Summons, R. E., Smith, K., Elvert, M., Hinrichs, K.: Intact polar membrane lipids in prokaryotes  
 and sediments deciphered by high-performance liquid chromatography/electrospray ionization multistage  
 mass spectrometry—new biomarkers for biogeochemistry and microbial ecology, *Rapid Commun. Mass  
 Spectrom.*, 18(6), 617–628, doi: https://doi.org/10.1002/rcm.1378, 2004.
55. Talbot, H. M., Bischoff, J., Inglis, G. N., Collinson, M. E. and Pancost, R. D.: Polyfunctionalised bio- and  
 geohopanooids in the Eocene Cobham Lignite, *Org. Geochem.*, 96, 77–92,  
 doi:10.1016/j.orggeochem.2016.03.006, 2016.
56. Thamdrup, B., Dalsgaard, T., Jensen, M. M., Ulloa, O., Farías, L. and Escobedo, R.: Anaerobic ammonium  
 oxidation in the oxygen-deficient waters off northern Chile, *Limnol. Oceanogr.*, 51(5), 2145–2156,  
 doi:10.4319/lo.2006.51.5.2145, 2006.
57. Van de Graaf, A. A., Mulder, A., De Bruijn, P., Jetten, M. S. M., Robertson, L. A. and Kuenen, J. G.:  
 Anaerobic oxidation of ammonium is a biologically mediated process, *Appl. Environ. Microbiol.*, 61(4),  
 1246–1251, doi:10.1128/aem.61.4.1246-1251.1995, 1995.
58. Van De Graaf, A. A., De Bruijn, P., Robertson, L. A., Jetten, M. S. M. and Kuenen, J. G.: Metabolic pathway  
 of anaerobic ammonium oxidation on the basis of <sup>15</sup>N studies in a fluidized bed reactor, *Microbiology*,  
 143(7), 2415–2421, doi:10.1099/00221287-143-7-2415, 1997.
59. Van De Vossenberg, J., Rattray, J. E., Geerts, W., Kartal, B., Van Niftrik, L., Van Donselaar, E. G.,  
 Sinninghe Damsté, J. S., Strous, M. and Jetten, M. S. M.: Enrichment and characterization of marine  
 anammox bacteria associated with global nitrogen gas production, *Environ. Microbiol.*, 10(11), 3120–3129,  
 doi:10.1111/j.1462-2920.2008.01643.x, 2008.



60. van Dongen, B. E., Talbot, H. M., Schouten, S., Pearson, P. N. and Pancost, R. D.: Well preserved Palaeogene and Cretaceous biomarkers from the Kilwa area, Tanzania, *Org. Geochem.*, 37(5), 539–557, doi:10.1016/j.orggeochem.2006.01.003, 2006.
61. Villanueva, L., Speth, D. R., van Alen, T., Hoischen, A. and Jetten, M. S. M.: Shotgun metagenomic data reveals significant abundance but low diversity of “*Candidatus Ca. Scalindua*” marine anammox bacteria in the Arabian Sea oxygen minimum zone, *Front. Microbiol.*, 5(31), 1–9, doi:10.3389/fmicb.2014.00031, 2014.
62. Wakeham, S. G., Amann, R., Freeman, K. H., Hopmans, E. C., Jørgensen, B. B., Putnam, I. F., Schouten, S., Sinninghe Damsté, J. S., Talbot, H. M. and Woebken, D.: Microbial ecology of the stratified water column of the Black Sea as revealed by a comprehensive biomarker study, *Org. Geochem.*, 38(12), 2070–2097, doi:10.1016/j.orggeochem.2007.08.003, 2007.
63. Woebken, D., Lam, P., Kuypers, M. M. M., Naqvi, S. W. A., Kartal, B., Strous, M., Jetten, M. S. M., Fuchs, B. M. and Amann, R.: A microdiversity study of anammox bacteria reveals a novel *Candidatus Ca. Scalindua* phylotype in marine oxygen minimum zones, *Environ. Microbiol.*, 10(11), 3106–3119, doi:10.1111/j.1462-2920.2008.01640.x, 2008.
64. Yang Y., Li M., Li H., Li X.Y., Lin J.G., Denecke, M. and Gu J.D. Specific and effective detection of anammox bacteria using PCR primers targeting the 16S rRNA gene and functional genes. *Sci Total Environ.*, 10, 734:139387. doi: 10.1016/j.scitotenv.2020.139387, 2020.